МІНІСТЕРСТВО ОСВІТИ ТА НАУКИ УКРАЇНИ
НАЦІОНАЛЬНИЙ АВІАЦІЙНИЙ УНІВЕРСИТЕТ
КАФЕДРА КОНСТРУКЦІЇ ЛІТАЛЬНИХ АПАРАТІВ

ДОПУСТИТИ ДО ЗАХИСТУ
Завідувач кафедри, к.т.н., доцент
_____ Святослав ЮЦКЕВИЧ
«____» _____ 2023 р.

КВАЛІФІКАЦІЙНА РОБОТА

ЗДОБУВАЧА ОСВІТНЬОГО СТУПЕНЯ «МАГІСТР»

ЗІ СПЕЦІАЛЬНОСТІ

«АВІАЦІЙНА ТА РАКЕТНО-КОСМІЧНА ТЕХНІКА»

Тема: «Ударні пошкодження армованих вуглецевим волокном пластиків»

Виконавець: _____ **Ніна РОГОЖИНА**

Керівник: к.т.н., доцент _____ **Олег ШЕВЧЕНКО**

Консультанти з окремих розділів пояснювальної записки:
охорона праці:
к.т.н., доцент _____ **Катерина КАЖАН**

охорона навколишнього середовища:
к.т.н., професор _____ **Леся ПАВЛЮХ**

Нормоконтролер: к.т.н, доцент _____ **Володимир КРАСНОПОЛЬСКИЙ**

Київ 2023

MINISTRY OF EDUCATION AND SCIENCE OF UKRAINE
NATIONAL AVIATION UNIVERSITY
DEPARTMENT OF AIRCRAFT DESIGN

PERMISSION TO DEFEND
Head of the department,
PhD, associate professor
_____ Sviatoslav YUTSKEVYCH
"___" _____ 2023

QUALIFICATION PAPER

FOR A MASTER'S DEGREE

ON SPECIALITY

"AVIATION AND AEROSPACE TECHNOLOGIES"

Topic: "Impact damage of carbon fibre reinforced plastics"

Fulfilled by:	_____	**Nina ROHOZHYNA**
Supervisor: **PhD, associate professor**	_____	**Oleh SHEVCHENKO**
Labor protection advisor: **PhD, associate professor**	_____	**Katerina KAZHAN**
Environmental protection adviser: **PhD, associate professor**	_____	**Lesya PAVLYUKH**
Standards inspector **PhD, associate professor**	_____	**Volodymyr KRASNOPOLSKII**

Kyiv 2023

НАЦІОНАЛЬНИЙ АВІАЦІЙНИЙ УНІВЕРСИТЕТ

Аерокосмічний факультет
Кафедра конструкції літальних апаратів
Освітній ступінь «Магістр»
Спеціальність 134 «Авіаційна та ракетно-космічна техніка»
Освітньо-професійна програма «Обладнання повітряних суден»

ЗАТВЕРДЖУЮ
Завідувач кафедри, д.т.н, доцент
_____ Святослав ЮЦКЕВИЧ
«_____» _____ 2023 р.

ЗАВДАННЯ

на виконання кваліфікаційної роботи здобувача

РОГОЖИНОЇ НІНИ ОЛЕКСІЇВНИ

1. Тема роботи: «Ударні пошкодження армованих вуглецевим волокном пластиків», затверджена наказом ректора від 20 вересня 2023 року № 1853/ст.
2. Термін виконання роботи: з 25 вересня 2023 р. по 31 грудня 2023 р.
3. Вихідні дані до роботи: вуглепластикові зразки, каталог матеріалів Hexcel.
4. Зміст пояснювальної записки: вступ, оглядова частина, що містить класифікацію та наслідки ударних випробувань композиційних матеріалів, попередні методи досліджень та вибірка для випробувань на низько швидкосний удар, порівняння симуляції з експериментальними даними, окремі розділи, присвячені питанням охорони праці та навколишнього середовища.
5. Перелік обов’язкового графічного (ілюстративного) матеріалу: результати симуляції удару, фото обох сторін вуглепластикових зразків після ударних випробувань.

6. Календарний план-графік:

№	Завдання	Термін виконання	Відмітка про виконання
1	Огляд літератури за проблематикою роботи. Аналіз впливу ударних випробувнь на вуглепластик.	25.09.2023–01.10.2023	
2	Проведення аналізу екпериментальних даних.	02.10.2023–15.10.2023	
3	Виконання та аналіз симуляції низькогвидкісного удару, порівняльний аналіз результатів.	16.10.2023–15.11.2023	
4	Виконання частин, присвячених охороні навколишнього середовища та охорони праці.	16.11.2023–26.11.2023	
5	Написання пояснювальної записки.	27.11.2023–03.12.2023	
6	Перевірка, редагування та виправлення пояснювальної записки.	03.12.2023–10.12.2023	
7	Подача роботи для перевірки на плагіат.	11.12.2023–17.12.2023	
8	Попередній захист кваліфікаційної роботи.	20.12.2023–24.12.2023	
9	Захист кваліфікаційної роботи.	25.12.2023–31.12.2023	

7. Консультанти з окремих розділів:

Розділ	Консультант	Дата, підпис	
		Завдання видав	Завдання прийняв
Охорона праці	к.т.н., доцент Катерина КАЖАН		
Охорона навколишнього середовища	к.т.н, професор Леся ПАВЛЮХ		

8. Дата видачі завдання: 25 вересня 2023 року

Керівник дипломної роботи _____ Олег ШЕВЧЕНКО

Завдання прийняв до виконання _____ Ніна РОГОЖИНА

NATIONAL AVIATION UNIVERSITY

Aerospace Faculty
Department of Aircraft Design
Educational Degree "Master"
Specialty 134 "Aviation and Aerospace Technologies"
Educational Professional Program "Aircraft Equipment"

APPROVED BY
Head of the department,
PhD, associate professor
_____ Sviatoslav YUTSKEVYCH
"___" _____ 2023

TASK

for the qualification paper

NINA ROHOZHYNA

1. Topic: «Impact damage of carbon fibre reinforced plastics», approved by the Rector's order № 1853/ст from 20 September 2023.
2. Period of work: since 25 September 2023 till 31 December 2023.
3. Initial data: carbon fibre reinforced plastics, Hexcel prepreg mechanical properties catalogue.
4. Content: introduction, overview section containing impact testing classification and effects of composite materials, preliminary analysis methods and sampling study for low-velocity impact testing, experimental data to simulation comparison, separate sections dedicated to labor protection and environmental protection.
5. Required material: impact simulation results, photographs of indentations on both sides of the specimens after impact.

6. Thesis schedule:

№	Task	Time limits	Done
1	Review of the literature on the issues of work. Analysis of carbon fibre reinforced plastics impact damage resistance.	25.09.2023–01.10.2023	
2	Processing of experimental data and material properties.	02.10.2023–15.10.2023	
3	Execution of low-velocity impact simulation, comparative results analysis.	16.10.2023–15.10.2023	
4	Execution of the parts, devoted to environmental and labor protection.	16.11.2023–26.11.2023	
5	Writing the report note.	27.11.2023–03.12.2023	
6	Report note checking, editing and correction.	03.11.2023–10.12.2023	
7	Submission of the work for plagiarism check.	11.12.2023–17.12.2023	
8	Preliminary qualification paper defense.	20.12.2023–24.12.2023	
9	Defense of the qualification Paper.	25.12.2023–31.12.2023	

7. Special chapter advisers:

Chapter	Adviser	Date, signature	
		Task issued	Task received
Labor protection	PhD, associate professor Kateryna KAZHAN		
Environmental protection	PhD, associate professor Lesia PAVLYUKH		

8. Date of issue of the task: 25 September 2023

Supervisor: _____ Oleh SHEVCHENKO

Student: _____ Nina ROHOZHYNA

РЕФЕРАТ

Кваліфікаційна робота «Ударні пошкодження армованих вуглецевим волокном пластиків» містить:

74 сторінки, 25 рисунків, 6 таблиць, 54 літературних посилань, 1 додаток (4 ст.)

В роботі були встановлені кількісні параметри пошкоджень вуглепластикових зразків з різним типом наповнювача при низькошвидкісному ударі, встановлено більш ударостійкий тип наповнювача, проведене моделювання ударних пошкоджень модельних зразків за допомогою програмного забезпечення, вперше досліджена релаксація пошкодження матеріалу за тижневий термін,.

В дослідницькій частині роботи для аналізу пошкоджень вуглепластиків при низькошвидкісному ударі були використані експериментальні та чисельні методи з використанням експериментальної установки для випробувань на удар та програмного забезпечення Abaqus/Explicit для моделювання та аналізу низькошвидкісного удару.

Результати цієї роботи можуть бути використані проєктуванні та виробництві деталей з вуглепластиків в місцях можливих ударних дій для різних галузей, вивчення релаксації вуглепластиків дозволить планувати терміни періодичних оглядів для виявлення ледь видимих пошкоджень від ударів.

Композиційні матеріали, вуглепластик, стійкість до пошкоджень, випробування на удар, низькошвидкісний удар, моделювання удару, релаксація матеріалу, ледь видиме ударне пошкодження

ABSTRACT

Qualification paper “Impact damage of carbon fibre reinforced plastics”

74 p., 25 fig., 6 tables, 54 references, appendix (4 p.)

In this work impact damage assessment of carbon fibre reinforced plastics with different filler type was conducted, damage resistant filler type was determined, low0velocity impact was simulated using the specialized software, for the first time material damage relaxation was determined over a weekly period.

In the research part of the work, experimental and numerical analysis methods such as Abaqus/Explicit software modelling, simulation and strength assessment were used for damage assessment and performance of carbon fibre reinforced plastics after low-velocity impact.

The results of this work can be used in production of carbon fibre reinforced plastic components in areas susceptible to impacts across various industries, the investigation of carbon fibre reinforced plastics damage relaxation will help facilitate periodic inspections scheduling to detect barely visible damages resulting from impacts.

Composite materials, CFRP, damage resistance, drop-weight impact test, low-velocity impact testing, impact simulation, stress relaxation, barely visible impact damage

CONTENT

ABBREVIATIONS

BVID – Barely Visible Impact Damage

CAI – Compression-after-impact

CFRP – Carbon Fibre Reinforced Plastic

CM – Composite Material

FE – Finite Element

FEA – Finite Element Analysis

FRP – Fibre Reinforced Plastic

HRC – Hardness Rockwell C Scale

LED – Light Emitting Diode

LVI – Low-velocity impact

NDI – Non-destructive Inspection

PCM – Polymer Composite Material

PICS – Post Impact Compressive Strength

PPE – Personal Protective Equipment

INTRODUCTION

In advanced military aircraft structures as well as passenger aircraft such as Boeing 787 and Airbus 350, the adoption of modern composite materials (CM) has largely supplanted conventional metals alloys. The structures mainly being: fuselage sections, wing structures empennage, landing gear and interior components. CM structures account for 50% or more of the total weight, resulting in significant enhancements in overall efficiency. Currently, weight optimization remains one of the most crucial tasks of the technical excellence of aviation and aerospace products. Addressing this issue, the application of polymer composite materials (PCM) plays a vital role. Aircraft structures made of PCM are much more technologically advanced than their metal counterparts, offering reduced weight.

However, they do entail higher mass manufacturing costs, so maintaining structural integrity throughout their operational lifespan becomes essential. Among the most commonly employed PCMs in aircraft structures, carbon fibre reinforced plastics (CFRP) stand out for their exceptional stiffness and lightweight attributes. Nonetheless, their vulnerability to impact damage during operation mandates a thorough investigation into the stability of PCMs, particularly CFRP. The damage stained after impact rarely visible but causes internal delaminations or cracks which in turn lead to reduction in strength, therefore shortening operational life.

This study is dedicated to experimental evaluation of low-velocity impact resistance of five distinct variants CFRP specimens in accordance with ASTM D7136/D7136-05 standard, with constant energy per unit thickness. Performed on the provided impact resistant Hexcel HexPly prepregs, that differ in epoxy matrix binder and reinforcement structure, specifically bidirectional carbon fibre and unidirectional carbon fibre band. The research focuses on examining the diameter and depth of damages caused by striker impacts, as well as investigating stress relaxation following a 7-day post-impact exposure period. Additionally, showcasing the capability to measure the internal stress and deformation by means of modelling in Abaqus software.

PART 1. IMPACT TESTING OF COMPOSITE MATERIALS

Aviation structures often experience various types of impacts during operation, which can be categorized into three types: high-velocity (energy) impacts that occur with significant acceleration and result in punctures; medium-velocity impacts that cause substantial damage without penetrating the structure; and low-velocity free fall impacts that leave dents and residual internal stresses in the material. As such the low-velocity drop weight impact test asserts impact resistance and structural integrity of various CM under realistic operational conditions as well as allows for the detection and characterization of hidden impact damage that may compromise the material's performance.

Significant damage to the reverse side of carbon fibre reinforced plastics (CFRP) highlights the relevance of investigating low-energy PCM impact damage. Barely visible damage occurring under free fall weigh drop on the front surface has a specific designation as a Barely Visible Impact Damage (BVID).

Susceptibility to damage from concentrated out-of-plane impact forces is one of the major design concerns of many structures made of advanced composite laminates. Knowledge of the damage resistance properties of a laminated composite plate is useful for product development and material selection. To establish quantitatively the effects of stacking sequence, fibre surface treatment, variations in fibre volume fraction, and processing and environmental variables on the damage resistance of a particular composite laminate to a concentrated drop-weight impact force or energy [1].

In metal structures, impact damage is typically considered less concerning due to the material's ductile nature, allowing for significant energy absorption. The material can undergo large strains at constant yield stress before work hardening, offering a level of resilience. In contrast, composites exhibit a wide range of failure modes and are susceptible to BVID, which significantly compromises structural integrity. Unlike metals, composites, being predominantly brittle, can only absorb energy through elastic deformation and damage mechanisms, lacking the ability for plastic deformation.

The concept of damage resistance in composites pertains to the extent of impact-induced damage in the material system. Notably, the majority of impacts on a composite

plate occur in the transverse direction, where the lack of through-thickness reinforcement results in notably poor transverse damage resistance. Interlaminar stresses, such as shear and tension, often trigger initial failure due to their comparatively low strengths in the interlaminar regions. Consequently, design considerations include employing failure strains of 0.5% as a safeguard against impact failure, which regrettably underutilizes the excellent in-plane strength and stiffness properties inherent to composites.

The purpose of conducting low-velocity impacts (LVI) coupon level tests is twofold: first, to assess parameters at the design phase, including the delamination threshold load, and second, to address safety concerns by establishing a correlation between internal damage and the depth of indentation.

Low-velocity impacts inflicted upon composite laminates raise notable safety concerns due to their capacity to induce substantial structural damage, notably delaminations and matrix cracking. These damages are often challenging to detect through visual inspections.

1.1. Low-velocity drop weight impact testing standards

The categorization of impacts is generally divided into low or high-velocity, with some disagreement among researchers regarding their precise definition. Low-velocity impacts are generally characterized as quasi-static events, with the upper time limit ranging from one to tens of milliseconds depending on factors such as target stiffness, material properties, and the mass and stiffness of the impacting object.

In contrast, high-velocity impacts are characterized by the dominant propagation of stress waves through the material, with the structure unable to respond adequately, resulting in localized damage. Boundary condition effects are negligible as the impact event concludes before stress waves reach the structure's edge.

In the case of low-velocity impacts, the dynamic response of the target structure becomes crucial as the contact duration allows for the entire structure to respond, thereby absorbing more energy elastically. Conversely, high-velocity impacts are characterized by fibre breakage induced by penetration, while low-velocity impacts result in delaminations and matrix cracking.

According to ASTM D7136 standard a drop-weight impact test is conducted using a balanced, symmetric laminated plate. The test involves applying concentrated out-of-plane impact on the plate using a drop weight equipped with a hemispherical striker tip. The resulting damage in the specimen is quantified to evaluate its resistance to damage. It is important to note that the response to damage is influenced by various factors such as test configuration, test conditions, and other variables. To ensure meaningful comparisons, identical test configurations and conditions must be employed when comparing different materials.

Optional procedures for recording impact velocity and applied contact force versus time history data are available. It is preferred that the impact-induced damage occurs in the central region of the plate, away from the plate edges, to prevent interaction between local stress states at the edges and the impact location during damage formation.

The susceptibility of advanced composite laminates to damage from concentrated out-of-plane impact forces is a significant design consideration for many structures. Understanding the damage resistance properties of laminated composite plates is valuable for product development and material selection.

The drop-weight impact test serves several purposes: quantifying the effects of stacking sequence, fibre surface treatment, variations in fibre volume fraction, and processing and environmental variables on the damage resistance of a specific composite laminate; comparing the damage resistance parameters of composite materials with different constituents; and inducing damage in specimens for subsequent damage tolerance tests.

The properties obtained through this test method provide guidance regarding the expected damage resistance capability of similar composite structures in terms of material, thickness, stacking sequence, etc. However, it is essential to recognize that the damage resistance of a composite structure is highly dependent on various factors including geometry, thickness, stiffness, mass, support conditions, etc. Significantly different relationships between impact force/energy and resultant damage state can arise due to variations in these parameters. For instance, the properties obtained using this test method are more representative of the damage resistance characteristics of an unstiffened monolithic skin or web rather than a skin attached to a substructure that resists out-of-plane

deformation. Similarly, the properties of the test specimen would be expected to resemble those of a panel with similar length and width dimensions rather than a significantly larger panel, which tends to redirect a greater proportion of the impact energy into elastic deformation.

The standard impactor used in the test has a blunt, hemispherical striker tip. Historically, this impactor geometry has exhibited more internal damage for a given amount of external damage compared to sharp striker tips in similar impacts. Alternative impactors may be suitable depending on the specific damage resistance characteristics being investigated. For example, sharp striker tip geometries may be appropriate for assessments related to damage visibility and penetration resistance. In other regard to this topic, a couple of researchers (Israr, Hongkarnjanakul, Rivallant, Bouvet) suggested in their fundamental article Post-Impact Investigation of CFRP Laminated Plate [2]:

- generally, the indentation just after the test, which is the temporary indentation, is always bigger than the indentation after a certain period due to the relaxation of the impacted composites;
- indentation depth decreased due to relaxation of the specimen and it has become almost constant after 48 hours of the tests;
- from the microscopic observations, this may be due to the existing of debris in the crack areas that tend to prevent the broken fibres and matrixes back their initial location.

The response of a laminated plate specimen to out-of-plane drop-weight impact is influenced by various factors including laminate thickness, ply thickness, stacking sequence, environment, geometry, impactor mass, striker tip geometry, impact velocity, impact energy, and boundary conditions. Consequently, valid comparisons between materials can only be made when identical test configurations, test conditions, and laminate configurations are used.

The impactor should have a mass of 5.5±0.25 kg and a smooth hemispherical striker tip with a diameter of 16±0.1 mm and a hardness of 60 to 62 HRC as specified in Test Methods E18. Alternative impactors may be employed to study the relationship between

visible damage geometry (e.g., dent depth, dent diameter) and the internal damage state. If a different impactor is utilized during testing, its shape, dimensions, and mass should be noted, and the results reported as non-standard.

It is recommended to test a minimum of five specimens per test condition unless valid results can be obtained with fewer specimens, such as in designed experiments. For comparative screening of drop-weight impact damage resistance of different materials, the standard specimen thickness should be within the range of 4.0 to 6.0 mm with a target thickness of 5.0 mm. The specimen thickness obtained in this study ranges from 2.09 to 3.04 mm.

1.2. Assessment of impact effects on composite structural performance

Low-velocity impacts can be defined as events which can occur in the range 1–10 m/s depending on the target stiffness, material properties and the projectile mass and stiffness [3]. A low-velocity impact event can occur in-service or during maintenance activities and can be considered one of the most dangerous loads on composite laminates. They jeopardize the performance of composites, rendering them an unsafe.

Pendulum-based testing methods such as the Charpy test, Izod test, drop towers, and drop weight test have become standard practices to conduct low-velocity impacts [4]. A drop weight impact testing unit realizes the simulation of diverse real-world impact conditions and facilitates the collection of detailed performance data. A notable advantage of this test, in comparison to the Charpy and Izod tests, lies in its capability to examine a wider range of test geometries, enabling the evaluation of complex components.

Multiple techniques exist for testing composites using low-velocity impact testing. The Charpy and Izod impact tests are commonly employed for comparing the impact response of isotropic materials with different compositions or manufacturing conditions. While both tests utilize a pendulum, the Charpy impact test supports the specimen as a simple beam, whereas the Izod impact test supports it as a cantilever. The ease of setup and the ability to rapidly collect substantial amounts of data are advantages of Izod and Charpy impact testing. However, the insights obtained from these tests lack depth in terms of revealing the material's characteristics. Nonetheless, researchers have made advancements

in utilizing Charpy impact tests to observe crack propagation, accurately measure force using high-speed photography, and obtain more comprehensive results.

Fibre composites are susceptible to delamination due to their low intralaminar strength. Interlaminar stresses arise in the boundary layer of laminates under transverse loading. The polymeric matrix within the material facilitates energy absorption and enables it to withstand impact energy. Low-velocity impact events do not result in perforation but induce delamination between layers without causing visible surface damage. Delaminations can also occur in the material during the industrial process due to factors like contaminated reinforcing fibres, inadequate fibre wetting, machining, mechanical loading, and insufficient reinforcement in the thickness direction [5].

Several parameters influence failure modes in composites subjected to low-velocity impact loading conditions, including fibre type, resin type, lay-up configuration, specimen thickness, impact velocity, and projectile type. Metals exhibit energy absorption in both elastic and plastic regions, whereas composite laminates primarily absorb energy through elastic deformation. Since most composites possess a brittle nature, they absorb energy through elastic deformation and damage mechanisms rather than plastic deformation.

During various stages of flight, such as take-off and landing, aircraft structures and equipment, including radar antenna, landing lights, canopy, windshield, lateral section or intake of the engine nacelle, turbine blades, and leading edges of the wing or tail empennage, are exposed to high-velocity impacts. Bird strikes represent a significant cause of such impacts due to their frequent occurrence and potential consequences [6]. The high relative velocities between an aircraft and a bird during a strike can result in instantaneous damage and failure of the aircraft's materials. To simulate this scenario, high-velocity impact testing is employed, which induces more severe damages that could lead to immediate material failure.

Structural survivability against high-speed projectile impacts is crucial in various applications. In aircraft and land-based vehicles, composites are utilized and designed to withstand high-speed impacts from components of damaged engines, turbine blades, and other debris. These materials are expected to possess high resistance to penetration by high-velocity projectiles. Impact refers to the collision between two or more bodies, while a

projectile is any object being launched. The target refers to a stationary or moving object that can be struck by the projectile.

Previous research has focused on investigating the penetration and perforation of Fibre Reinforced Polymer (FRP) laminates using various projectile shapes, such as flat-faced, hemispherical ended, conical-tip, and truncated-cone-nose projectiles, in high-velocity impact tests. Most of these impact tests have been conducted on thin laminates, typically with a thickness not exceeding 2 or 3 mm.

For high-velocity impact testing, the velocities of the projectiles depend on the pressure exerted by the gas gun. However, for low-velocity impact testing, the velocity of the drop mass depends on the height of the drop mass. It was found that CFRP plates show the best structural performance under low-velocity impacts, and for high-velocity impacts, a hybrid composite that contained carbon/glass fibre shows the best structural performance [7]. For low-velocity impact loading, the magnitude of the impact velocity influences the contact force and deflection of the sandwich structure. The peak force increased with increasing impact velocity. In ballistic impacts (short contact between impactor and target) the damage is localized and clearly visible by external inspection, while a low-velocity impact involves a long contact time between the impactor and target, which produces global structure deformation with undetected internal damage at points far from the contact region.

1.3. Performance of composite materials under drop-weight testing

A fibre-reinforced composite material comprises two primary components: reinforcement (filling such as fibres or other), matrix; and the interphase region of fibres and matrix bond. The properties of these constituents play a significant role in determining the threshold energies or stresses required for initiating various failure modes caused by impacts. The fibres act as the primary load-bearing element, contributing to the majority of the composite's strength and stiffness. Common fibre types include glass, carbon, and Kevlar (para-aramid), each exhibiting distinct characteristics. Carbon fibres, renowned for their high strength, light weight and stiffness, are extensively employed in aerospace structures. However, they possess brittleness with limited strain-to-failure relation (0.5% to 2.4%). Glass fibres, on the other hand, offer lower strength and stiffness but exhibit a higher strain-

to-failure relation (~3.2%) and are comparatively more cost-effective than carbon fibres. Kevlar fibres fall somewhere between carbon and glass in terms of mechanical properties. Despite carbon fibre's exceptional attributes, susceptibility to impact-related stress restricts the full utilization of its superior performance. In the context of low-velocity impact resistance, the capacity to store energy elastically within the fibres is a crucial parameter, primarily influenced by the fibre modulus and failure strain. E-glass fibres, for instance, can absorb approximately three times more elastic energy than carbon fibres. Hybrid composites, which combine carbon with glass or Kevlar fibres, are often employed to enhance impact resistance. However, the mismatch in modulus between different fibre types introduces complexities in hybrid composite design.

In FRP, the polymer matrix, typically a thermoset material, serves various critical functions. It transfers loads to the fibres, shields them from self-damage, and aligns/stabilizes the fibres. Epoxy resins are commonly employed in structural applications due to their ability to meet hot/wet compressive strength requirements. However, epoxy exhibits brittleness and poor resistance to crack propagation, specifically delamination. Efforts to enhance the interlaminar fracture toughness and reduce matrix damage in thermoset resins have involved the inclusion of plasticizing modifiers or incorporating rubber or thermoplastic particles into the resin. Nevertheless, improvements in interlaminar fracture toughness typically result in trade-offs with mechanical properties, and enhancements made to the pure matrix do not fully translate to the composite due to the presence of brittle fibres that inhibit the growth of plastic zones within the matrix. Another approach to mitigate delamination is the incorporation of a thin layer of highly resilient resin with excellent shear strain capabilities.

Alternatively, the use of thermoplastic resins, such as poly(ether-ether-ketone), can significantly enhance fracture toughness by an order of magnitude compared to thermoset composites. However, challenges related to low thermal stability, chemical resistance, inadequate fibre-matrix interfacial bonding, and creep limitations have historically impeded the widespread adoption of thermoplastic composites. The utilization of thermoplastics in composite systems is still hindered by the need for novel production techniques, but as these

challenges are overcome, thermoplastic-based composites are becoming increasingly more competitive.

The interphase region between the fibre and matrix plays a crucial role. Carbon fibres are typically subjected to an oxidative treatment to enhance the adhesion between the fibre and matrix, whereas glass fibres are treated with a coupling agent. The quality of the interphase region can influence the specific failure mode that occurs under a given load. For instance, inadequate adhesion can lead to failure at low transverse stress levels, resulting in clean fibres. The bond strength within the interphase can be adjusted to improve toughness by facilitating energy absorption through fibre-matrix debonding. However, this adjustment inevitably leads to a reduction in overall mechanical properties.

The inherent heterogeneity and anisotropic characteristics of FRP laminates contribute to the occurrence of four primary modes of failure:

- matrix mode: involves cracking that transpires parallel to the fibres, resulting from tension, compression, or shear stresses;
- fibre mode: tensile loading leads to fibre breakage and/or pull-out, while compressive loading causes fibre buckling;
- delamination mode: interlaminar stresses induce the formation of delamination, where adjacent layers separate from each other;
- penetration: impactor fully penetrates the surface, resulting in complete perforation.

The majority of impact test studies documented in the literature have primarily focused on low-energy testing, typically ranging from approximately 1 to 5 J, which results in minimal damage.

Such investigations have provided insights into the initiation of matrix cracking and delamination. Matrix damage, primarily manifested as matrix cracking and fibre-matrix debonding, serves as the initial form of failure induced by transverse low-velocity impacts. Matrix damage, arising from low-velocity transverse impacts, initially manifests as matrix cracking and debonding between the fibre and matrix [8]. Matrix cracks predominantly occur in unidirectional layers and are oriented parallel to the fibre direction. Notably, the

pattern of cracks and delaminations is as follows: shear cracks develop at approximately 45 degrees under the edges of the impactor in the upper and middle layers, induced by exceedingly high transverse shear stresses. Additionally, Eltaher, Basha, Wagih, Melaibari and Lubineau (2022) [9] warned that the delaminations at the lower part of the laminate initiate due to the high bending stresses, that causes high tensile stresses at the 0 plies while the 90 plies are less stressed, which results in delamination initiation due to mismatch of stresses concentration. Based on the microstructure observations, the damage is distributed through the whole thickness of the laminate and varying between matrix cracks and delamination. On the other hand, the cracks in the bottom layer, referred to as bending cracks, exhibit a vertical orientation and originates from elevated tensile bending stresses, closely associated with the flexural deformation of the laminate. It is crucial to emphasize that the specific type of matrix cracking observed is contingent upon the overall structure of the impacted specimens. For elongated and slender specimens, bending cracks occur in the lower layers due to excessive transverse deflection, accompanied by prevailing membrane effects. In contrast, shorter and thicker specimens exhibit higher stiffness, resulting in transverse shear cracks under the impactor in the upper plies when subjected to higher peak contact forces.

Delamination refers to a crack that occurs within the resin-rich region (typically around 0.0007 mm in graphite/epoxy laminates) between plies of varying fibre orientations, rather than between lamina of the same ply group [10]. The occurrence of delamination due to transverse impact is observed only once a specific threshold energy level is surpassed, and it has been noted that delamination typically takes place in the presence of a matrix crack. It has been found that delamination may deviate slightly from the exact interface region and propagate on either side. When the inclined shear crack in the upper layer reaches the interface, it is impeded by the change in fibre orientation, resulting in its propagation as a delamination between the layers. This delamination is usually restricted by the middle transverse crack. On the other hand, the initiation of the lower interface delamination is believed to be triggered by the vertical bending crack, with its growth being less constrained. Matrix cracks that lead to delamination are referred to as critical matrix cracks.

The propagation of delamination is governed by the interlaminar longitudinal shear stress and transverse in-plane stress exerted in the layer located below the delaminated interface, as well as by the interlaminar transverse shear stress experienced in the layer above the interface. To evaluate the growth of delamination from a known initial size, several researchers have introduced artificial delamination during the manufacturing process by incorporating a thin foil between plies. Through analysis, it was observed that there exists a linear correlation between the peak force applied and the area of delamination. By extrapolating from these findings, a threshold force value for the initiation of delamination was determined [11].

The fibre failure mode typically occurs at a later stage in the fracture process compared to matrix cracking and delaminations. However, research efforts have primarily focused on low-energy damage modes, resulting in limited information regarding fibre failure. Fibre failure arises as a consequence of locally elevated stresses and indentation effects, primarily governed by shear forces, in the region directly impacted by the external force. Additionally, on the non-impacted face, fibre failure occurs due to the presence of high bending stresses. Fibre failure serves as a precursor to the more severe catastrophic penetration mode.

Penetration is a macroscopic failure mode that occurs when fibre failure progresses to a critical extent, allowing the impactor to fully penetrate the material. Investigation of penetration impact has primarily focused on the ballistic domain, although some studies have explored low-velocity impacts. Findings have demonstrated a notable increase in the threshold of impact energy required for penetration with increasing specimen thickness in CFRP materials.

The main weakness of composite laminates in terms of residual properties is the low post-impact compressive strength (PICS). This weakness is mainly due to local instability caused by delamination, resulting in a significant reduction in compressive strength. Even low-energy impacts can induce delamination, resulting in significant loss of strength under pressure, especially in the case of barely visible impact damage (BVID). Delamination divides the laminate into partial laminates that have reduced bending stiffness compared to the original laminate, making them more susceptible to bending under compressive loads.

When subjected to compressive loads, delamination can cause buckling in one of three modes: global instability/buckling of the entire laminate, localized instability characterized by buckling of the thinner lower laminate, or a combination of the two. As the delamination length increases, the failure mode usually shifts from global to local and finally to mixed modes. PICS testing is often challenging because it requires a large enough measurement range to accommodate damage. It is worth to note that hybrid composites are found to be more prone to delamination [12].

Composite materials are susceptible to impact damage, which significantly reduces residual strength and structural integrity. The term damage tolerance refers to the ability of a system to function after an impact. Even BVID can cause up to 50% strength loss. Residual strengths in tension, compression, bending and fatigue will be reduced to varying degrees depending on the dominant damage mode [13].

1.4. Non-destructive post impact inspection of composite materials

After conducting a low-velocity impact test on CFRP materials, the implementation of non-destructive inspection (NDI) assessment emerges as a critical component of the evaluation process. Such inspections include but are not be limited to ultrasonic inspection, emission tomography scanning, shearography, terahertz imaging, thermography, x-ray radiography, microscopic inspection, digital holography. The first four methods are briefly covered in this chapter.

Composite laminates can develop internal defects from low-velocity impacts, which may not be visible. Ultrasonic testing is a common method for detecting and measuring such hidden damage. This non-destructive inspection technique uses high-frequency sound waves to penetrate the material and provides real-time monitoring, allowing for precise measurements of defect sizes and locations. This helps assess the structural integrity of CFRP materials comprehensively. Ultrasonic testing provides valuable insights into the post impact effects such as damage area dimensions and detected delaminations. A typical ultrasonic testing system consists of a transmitter and receiver circuit, transducer tool and display devices. By adopting the ultrasonic transducer, repeated ultrasonic pulses are introduced into a material, and resultant waveforms carry the morphological information

that contributes to damage mechanisms [14]. In [15] high resolution digital data and images from three sections of the specimen could be obtained: the in-plane section, and the two through-the-thickness sections by means of carried out inspection: by fixing the ultrasound gel covered specimen on a flat support and moving the ultrasonic probe manually along the specimen surface. However, ultrasonic scanning displays difficulty when assessing the damage size after cyclic loading, whereas a more in-depth C-scan provides a more comprehensive visual representation of the distribution and severity of defects [12,16], although without specifying the nature and location of the damage [17].

Shearography is a specialized optical technique for identifying and quantifying surface damages. This NDI method offers real-time, high-resolution imaging of surface deformations and defects. Shearography is remarkably resilient to environmental disturbances for an interferometric technique and is therefore better suited to operation in industrial environments where it has become well established, it is reliant on the laser speckle effect, which occurs whenever light with sufficient temporal and spatial coherence is scattered from an optically rough surface whose topographical features are greater than the wavelength of the light. When this occurs, a complex granular pattern is produced which is the result of the constructive and destructive interference of light scattered from different points on the surface [18]. Granular patterned imagery produced resembles relief contour lines for detected defects.

Terahertz imaging uses non-ionizing electromagnetic waves band to penetrate through the material [19]. In comparison to X-ray radiation, THz radiation is unharmful for people and may penetrate clothes. The THz produced imagery contains noises in a form of wide, alternating arranged lighter, and brighter areas, indicating the propagation of the electromagnetic wave in homogeneous medium [20]. THz imaging is a reliable NDI method provides real-time imaging of internal features, enabling a detailed assessment of the impact effects on CFRP while possessing similar flaws as C-scan method, e.g. small penetration depth due to limited frequency.

Conclusion to the Part 1

The utilization of composite materials has increased in aviation is continuously progressing. Composite materials in aircraft structures have numerous benefits, including reduced weight, superior resistance to corrosion, and increased resistance against fatigue-induced damage. These factors reduce the long-term cost of operation of the aircraft, which ultimately increases effectiveness. Notably, the composition and thickness of the material directly affect the behaviour of impacts. Additionally, factors like the weight, shape, elasticity, and angles of incidence of the projectile must be considered. The critical areas covered in this review encompass an introduction and classification of impact testing, and failure modes observed in composites.

Interlayer edge stresses due to applied in-plane loads can reduce the strength of the laminate and can increase under cyclic loading, causing a further reduction in the load-bearing capacity of the laminate. The onset of edge delamination is more likely to occur at low strain levels under in-plane tensile forces than under compressive loads. Nevertheless, delaminations from compressive loads are much more dangerous than those from tensile loads.

A higher velocity impact is predominantly associated with penetration of the structure (and shearing of reinforcing members), whereas a lower velocity impact is more likely to cause delamination.

PART 2. PRELIMINARY ANALYSIS METHODS AND SAMPLING STUDY FOR LOW-VELOCITY IMPACT TESTING

When designing any damage tolerant layered composite load bearing structures such common types of damage are considered: delaminations and complete penetrations. Operational experience has proven impact damage incidental in most cases. Although defects do not progressively grow to become widespread, systems subjected to continuous cyclic or alternating load have had the growth of these two types of damage eventually lead to fibre fracture which was the final cause of structural failure in [21]. The possible buckling of damaged laminate elements can result in reduced compressive strength as mainly shown in compression-after-impact (CAI) tests described in [22] and additional experimental testing at the ANTONOV enterprise. This work is carried out in order to predict damage severity upon impact and to establish the reliability of impact simulation - it's correspondence with experimental data. Thus, both simulation process, necessary experimental and measuring equipment description are featured in this part.

2.1. Sample preparation and material properties

Five coupon batches were manufactured from different Hexcel epoxy matrix based prepregs: 913/35%/UD132/HTS-12K, 913/46%/G18NT, M21/40%/268T2/AS4C-6K, M21/34%/UD194/IMA-12K, M21/34%/UD268/AS7-12K.

Laminate layups consisted of 16, 12, and 8 stacked number of plies, with varied nominal ply thickness due to normalized values 0.21-0.135 mm. Most prepreg plies were stacked in (-45/45, $[0]_4$, 45/-45) sequence while the 913/46%/G18NT prepreg coupons followed a (-45/45, $[0]_8$, 45/-45) sequence layup.

Three 913/35%/UD132/HTS-12K samples had 16 layers stacked in (-45/45, $[0]_4$, 45/-45) sequence; two 913/46%/G18NT samples had 12 layers with (-45/45, $[0]_8$, 45/-45) sequence; two M21/40%/268T2/AS4C-6K, M21/34%/UD268/AS7-12K and one M21/34%/UD194/IMA-12K samples had 8 layers and (-45/45, $[0]_4$, 45/-45) layup sequence.

The CFRP coupons batches were produced using vacuum bag in-autoclave process. The prepregs were laid up on a flat metal tool precoated with a release layer. Limiting strips

with a height equal to the stacked up plies thickness were installed along the contour of the tool acted as sealants to maintain pressure. Two layers of fiberglass T-13 drain cloth were placed on top of the stacks. Vacuum tubes were installed along the two large sides of the metal mould tool. The vacuum bag was made of TC bagging film. Then the vacuum-bagged laminate underwent curing in an autoclave.

According to the technical documentation of the supplier company Hexcel, prepreg components based on the M21 epoxy polymer matrix can be moulded using multiple curing processes, depending on their thickness and structure.

The in-autoclave curing process (Fig. 2.1) is designed for monolithic laminates with less than 15 mm thick consists of applying full vacuum of 0.1 MPa and pressure of 0.7 MPa. Then reducing vacuum to a safe value of -0.02 MPa when the autoclave pressure reaches ~ 0.1 MPa. Raising the temperature at 1-3 °C/min rate to 180±5 °C and dwelling 120±5 minutes, then cooling down at a 2-5 °C/min rate. Dropping the pressure completely when temperature cooldown reaches 60 °C, then performing a complete cooldown [23].

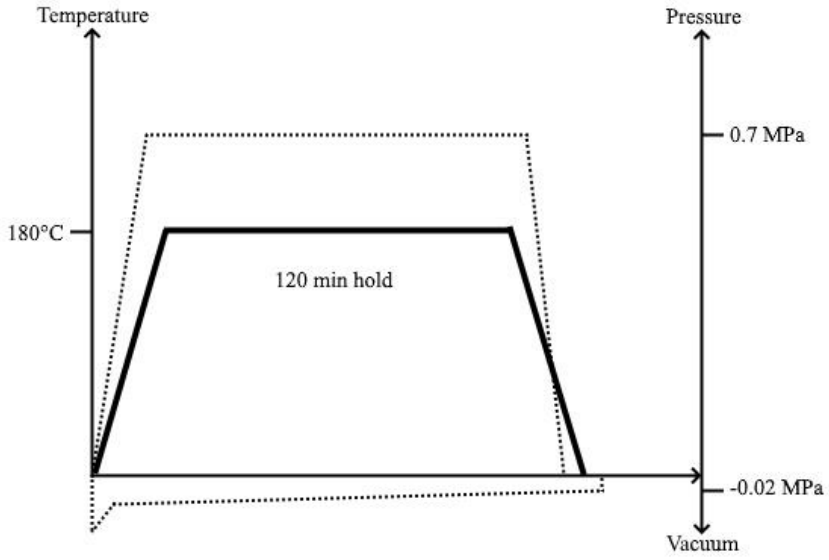

Fig. 2.1. In-autoclave moulding process for M21 prepreg.

Curing process of prepregs based on 913 epoxy matrix depends on the reinforcing fibre type: tape or fabric.

For unidirectional tape laminates, it is recommended, after applying full vacuum and

pressure of 7 MPa, to gradually raise the temperature at 1-3 °C/min to 125 °C. Then dwelling for 60 minutes, cooling down at 1-3° C/min rate to 60 °C and dropping the pressure before performing complete cooldown.

Fabric based laminates are cured under same applied vacuum but pressure variation between 0.3-0.7 MPa. Raising the temperature at a 2-3 °C/min rate and dwelling at 90 °C for 30 minutes and then at 125 °C for 60 minutes. Performing cooldown at a rate of 1-3 C/min to 60 °C and dropping the pressure. Later cooling down completely.

In addition to the primary curing mode 125° C for 60 minutes, several alternative are suggested:

- 130 °C dwell for 90 minutes;
- 140 °C dwell for 40 minutes;
- 150 °C dwell for 20 minutes;
- 160 °C dwell for 10 minutes.

Components up to 3 mm thick can be cured without a dwell in the schedule provided that the heat-up rate is not more than 5 °C/min. A dwell period is necessary in the heat-up to avoid the occurrence of a resin exotherm (usually 80 – 100 °C) but the dwell period will depend on the mass and type of tool [24].

Cured CFRP specimens were cut into coupons – rectangular 150 mm × 100 mm panels. The in-plane strengths and elastic moduli of the CFRP laminate used in the finite element (FE) model were obtained from the corresponding standard tests conducted in the Antonov enterprise laboratory of physical-chemical analysis and testing at the CM research department using testing machines such as Instron 5582, УМЕ – 10ТМ, 1958Y10. Impact testing was performed in the Department of Mechanics laboratory at NAU.

The samples were saturated with moisture. In distilled water for 30 days, after which the specimens were tested on an Instron 5582 testing machine using a thermal chamber at a temperature of +80°C. In determining the modulus of elasticity and Poisson's ratio, the following devices were used for strain measurement:

- a biaxial extensometer included in the Instron 5582 testing machine, which simultaneously records longitudinal and transverse deformations;
- an axial extensometer included in the Instron 5582 testing machine, which records

only longitudinal deformation;

- КФ5П1-5-200 type strain gauges were used, as the extensometers could not be employed.

To further expand the scope of analysis, that is – evaluation of the FE model and real experimental data comparability, Hexcel Catalogue prepreg properties were also in modelling a twin batch of FE models. Meaning that FE models possessed materials with mechanical properties based on Antonov Enterprise experimental data and Hexcel Corporation internal tests. Complete list of mechanical properties used in FE analysis of low-velocity impact is presented in table 2.1.

Table 2.1

Material Properties of Hexcel Catalogue Prepregs & Tested By Antonov Enterprise

	913/35%/UD132/HTS-12K Antonov	913/35%/UD132/HTS-12K Hexcle	913/46%/G814NT Antonov	913/46%/G814NT Hexcel	M21/40%/285/AS4C-6K Antonov	M21/40%/285/AS4C-6K Hexcel	M21/34%/UD268/AS7-12K Antonov	M21/34%/UD268/AS7-12K Hexcel	M21/34%/UD194/IMA-12K/300 Antonov	M21/34%/UD194/IMA-12K/300 Hexcel
Property	Results (average)									
Ult. Tensile Strength 0°, MPa	2093	2300	620	550	875	885	1923	1966	1843	2350
Tensile Young Modulus 0°, GPa	118.8	127	563.53	52	614.94	67.6	138.3	1491	164.87	148
Tensile Poisson Ratio 0°	0.285	-	0.061	-	0.058	-	0.340	-	0.342	-
Tensile Poisson Ratio 90°	-	-	0.0061	-	-	-	-	-	-	-
Ult. Tensile Strength 90°, MPa	39.7	-	525	-	769	-	49.4	1024	41.2	1024
Tensile Young Modulus 90°, Gpa	7.523	-	57.718	-	57.06	-	9.154	8.25	8.662	8.25
Ult. Compressive Strength 0°, MPa	1026	-	573	-	702	835	1305	1344	1199	1344
Ult. Compressive Strength 90°, MPa	168	-	469	-	674	-	225	796	213	1560
Compressive Young Modulus 90°, GPa	-	-	-	-	-	59.7	-	1272	-	123
Ult. In-plane Shear Strength, MPa	91.6	-	126.4	-	128	-	104	-	135	109
In-plane Shear Young Modulus, GPa	11.38	-	12	-	4.2	11.38	4.782	4.93	5.033	5.2
Ult. Interlayer Shear Strength 0°, MPa	78.8	81	69.3	60	66.2	70	102.6	103	101	144
Ult. Interlayer Shear Strength 90°, MPa	-	-	-	-	66.3	-	9.4	-	9.2	-

2.2. Impact simulation

The explicit impact was simulated in Abaqus software package using the FE method. Complete library of used materials with properties defined in table 2.1 was created pre-emptively for convenience. The methodology of simulation followed similar methodology to [25], general steps being: geometry modelling, definition of material properties and layup, interaction properties, mesh generation, boundary conditions, step and output management.

Firstly, a sketch of CFRP plate was created as a 3d deformable planar shell 100 mm in width and 150 mm in length (Fig. 2.2).

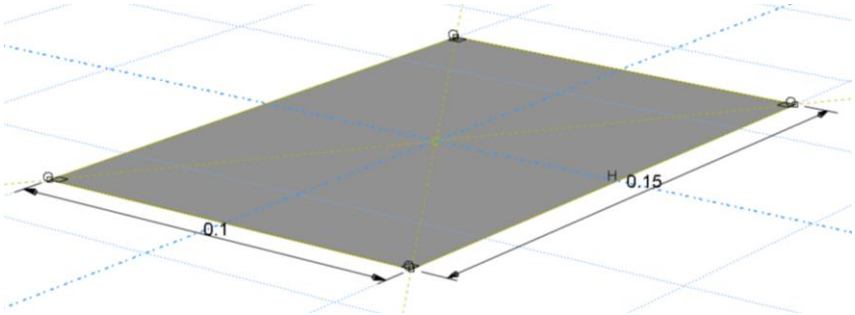

Fig. 2.2. CFRP plate sketch.

The striker tip sketch had discrete rigid properties and revolution shell type geometry creation with 16 mm in diameter and 10 mm in length (Fig. 2.3).

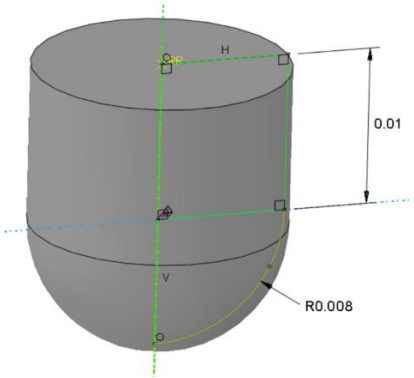

Fig. 2.3. Striker tip sketch.

Impactor was assigned standard steel material properties listed in table 2.2, and an

inertia node with the specified mass of 2.248 kg.

Table 2.2

Striker Material Properties

Striker tip	
Property	Steel
Young modulus, GPa	200
Poisons ratio	0.25
Density, kg/m^3	7.750
Mass, kg	2.248

CFRP plate was assigned a conventional shell layup section type. Number of layers, material and stacking sequence are comprehensively shown in table 2.3.

Table 2.3

Composite Section Properties

Plate			
Material	Number of plies	Ply thickness, mm	Ply Sequence, °
913/35%/UD132/HTS-12K	16	0.135	-45/45, [0]4, 45/-45
913/46%/G18NT	12	0.21	-45/45, [0]8, 45/-45
M21/40%/268T2/AS4C-6K	8	0.238	-45/45, [0]4, 45/-45
M21/34%/UD194/IMA-12K	8	0.39	45/45, [0]4, 45/-45
M21/34%/UD268/AS7-12K	8	0.25	-45/45, [0]4, 45/-45

The parts were then converted into an assembly, aligned and paired. The striker was assigned a rigid body interaction property, while the opposing outer surfaces (Fig. 2.4) of the plate and the tip were assigned a hard penalty contact interaction property with 0.3 friction coefficient. To avoid a common computational glitch that causes discrepancies overarching global property was set as frictionless.

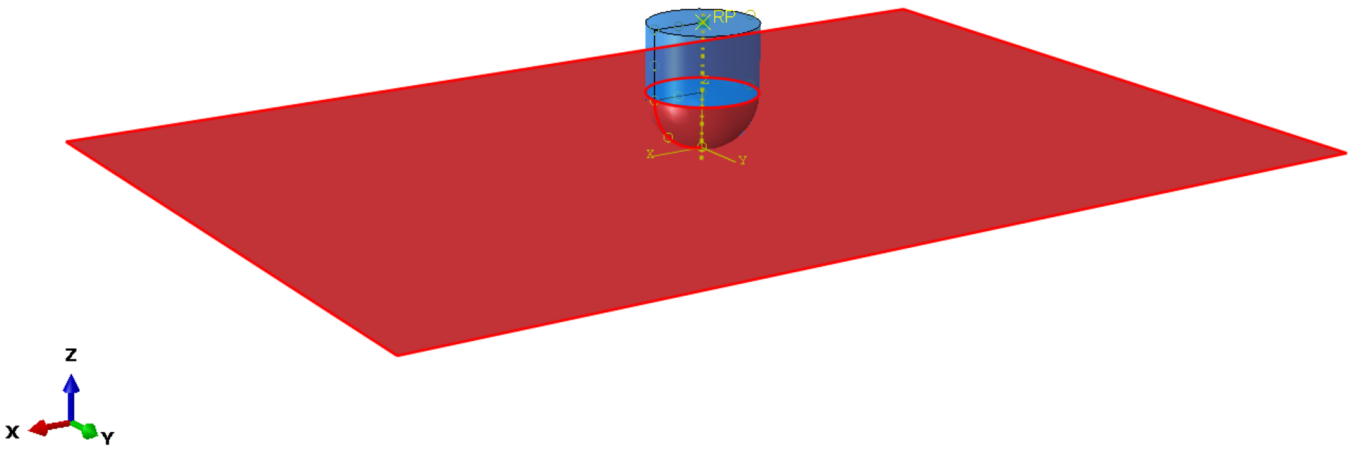

Fig. 2.4. Surfaces in contact.

A precise quadrilateral mesh was applied to the plate (seed size 3 mm), the striker was meshed with quadrilateral dominated path type (seed size 9 mm) shown in Fig. 2.5.

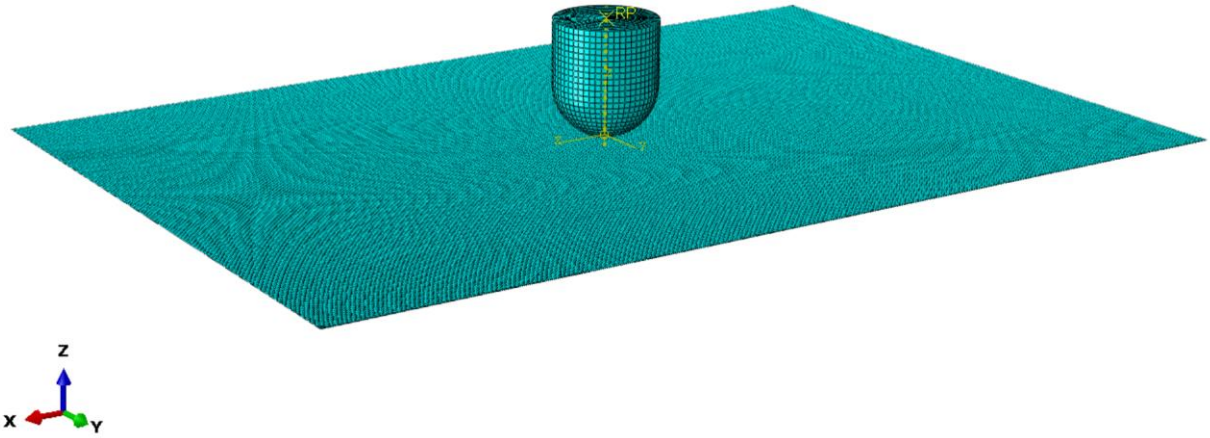

Fig. 2.5. Meshed parts.

In history output and field output manager the Energy, Displacement, Misses and Reaction Force values were selected and a force node was set. A dynamic explicit Step is then created. Time interval was set to $9.9 \cdot 10^{-5}$ s.

Boundary conditions such as drop velocity, and initial displacement lock were applied to striker tip. Rotary displacement lock served as a defined axis of movement and prevented the impactor from performing revolutions. The pinned boundary condition was applied to the four corners of the plate, allowing it to deform it keeping the edges in place. Such combination of boundary conditions ensures direct impact with specified velocity and

limited displacement solely along the Z-axis. Applied conditions are shown in Fig. 2.6.

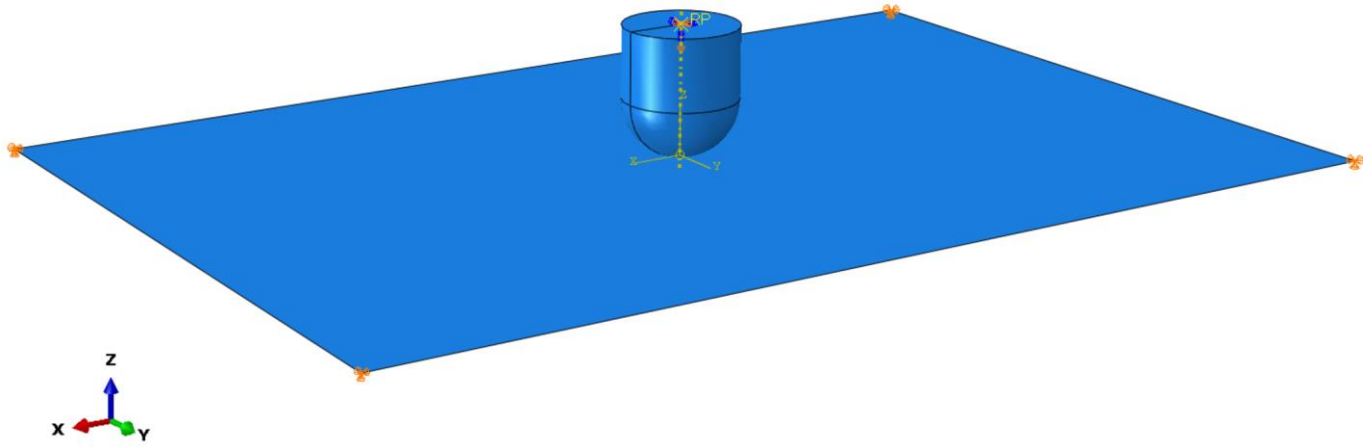

Fig. 2.6. Boundary conditions.

Finally the Finite Element Analysis (FEA) Jobs were submitted for analysis. The simulation results shall be highlighted along the experimental data in the next part of this thesis.

2.3. Impact testing installation overview

In accordance with applied ASTM D7136/D7136 M – 05 standard, damage is to be caused to the specimens by striking them with a falling weight with a determined energy. The obtained damage parameters are then measured. An experimental drop tower installation for these tests was designed and manufactured at the National Aviation University Department of Mechanics research laboratory.

The general view of the unit with the impactor is presented in the Fig. 2.7. The test specimen of 100 x 150 mm dimensions is fixed on the upper support part with a rectangular cut-out 75 x 125 mm of the rigid base support by means of special clamps with rubber tips. Damage is performed with the impactor being raised to a height that provides the required impact energy, with the defect parameters subsequently determined.

Fig. 2.7. Impact testing installation.

Three special stops limit the movement of the specimen until it is secured. The rubber tip clamps the sample onto the support slide, offset 6 mm from its end, axially symmetrical to the cutout in the rigid base. The distance between the centres of the grippers was 100 mm along the long side of the specimen and 87.5 mm along the short side (Fig. 2.8).

Fig. 2.8. Clamped specimen.

To ensure fixation of the specimen at the specified points, the clamping devices were bolted to the supporting slipway by fixing the clamping screws in a conductor (Fig. 2.9). The conductor is a steel plate with four precisely drilled holes. The clamping force according to the standard must be at least 120 kg and in order to ensure the specified clamping force of each tool head in each experiment, additional studies and tests were carried out, the results

of which are presented below, allowing to guarantee the specified clamping force of the tool heads.

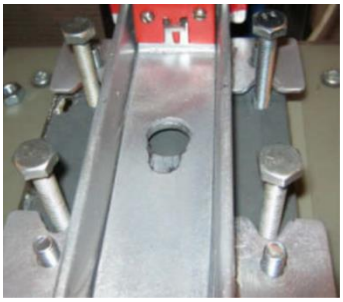

Fig. 2.9. Clamping conductor.

The first variant of the installation for testing specimens by falling weight impact was chosen from the standard, according to which the weight falls in a vertically fixed tube. The base of the drop tower is a repurposed drilling machine bed with a movable lower platform to which a rigid base with a cut-out for fixing specimens above with the help of special devices is attached (Fig. 2.10a). A rigid duralumin tube is vertically attached to the upper part of the bed. The 5 mm tube possesses a longitudinal slit, and an inner diameter of 31, serves as a guide for the falling weight (Fig. 2.10b).

(a) (b)

Fig. 2.10. Cut-out base (a) and vertical guide tube(b).

The impactor (striker) is of cylindrical shape structurally consisting of three threaded connected parts. The central part is a steel cylinder 30 mm in diameter which has a special

coating of shrink film to reduce the friction of the striker with the inner surface of the guide tube. This cylindrical part has internal threads on both sides: M12 on the bottom and M8 on top, respectively. A special tip - a striker with a spherical end is screwed to the bottom part. To the top - an aluminium alloy protruding rod, a long shank 8 mm in diameter, that allows lifting the weight and fixing it at different heights by means of a special clamping device.

In accordance with the requirements of the testing standard, the end of the falling weight must have a hemispherical shape with a diameter of 16x0.1 mm and a hardness of 60-62 HRC. In regard to the above, a 16 mm diameter bearing ball was chosen as the tip, which has a hardness not lower than the specified hardness and a very precise spherical shape. For the tests, a specially shaped shapely turned rod with an M12 thread on one side and a 16 mm diameter ball welded on the other side, with the protruding part measuring 6.5 mm is chosen (Fig. 2.11).

Fig. 2.11. Striker tip.

The impactor (falling weight) was lifted in the tube with a shank to a given lift height H. The impactor drop height (distance from the tip of the impactor to the specimen surface) was measured using a calliper complete with a 100 mm gauge and a special spacer. The entire measuring system is shown in the photo Fig. 2.12a.

The tip of the striker is brought to the top surface of the spacer and the striker is locked in position by a trigger mechanism. This trigger mechanism, which is shown in Fig. 2.12b, allows the striker to be held at a given height H above the samples and at the right moment allows the striker to be reset by pressing the horizontal lever.

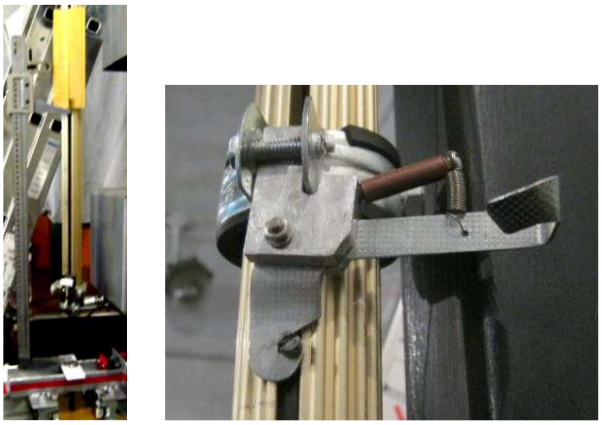

(a) (b)

Fig. 2.12. Measurement complex (a) and trigger mechanism (b).

Based on the requirements of the research methodology of inflicting only one indentation and blocking the possibility of another as a result of the impactor's rebound the specimen bed is equipped with a protective shield. A computerised electromechanical blocking system which would shield off the impact area of the test specimen after the initial one.

The electromechanical blocking system is controlled by a computer processing unit that receives striker position data from sensors relative to the test object. Previous studies and expert analysis have shown that the upward bounce of the striker after the damage ranges between 100 to 700 mm. Therefore in the case of an upward bounce of the striker and the repeated impact of no more than 0.1 mm was regarded as a single impact. The developed computerised electromechanical blocking system consists of four main parts:

- an electromechanical blade target cut-off system;
- a system of sensors evaluating the striker position relative to the specimen;
- computerised blocking control systems;
- power supply unit of the executive electromagnet.

The electromechanical cut-off system mounted on adjustable screws above the specimen is shown in Fig. 2.13. Overall it is comprised of a channel-like guide with a hole for the striker to pass through, on which a movable shaped cut-off blade and a powerful electromagnet are mounted.

Fig. 2.13. Electromechanical blocking system.

The movable shaped cut-off blade due allows to cut off the striker from the target upwards to a distance of at least 4 mm. The cut-off blade is activated by a powerful electromagnet. Inertial loads on the cut-off blade and the electromagnet core are damped by elastic elements mounted inside the electromagnet housing.

The electromagnet power supply unit is a powerful 5 kW battery-capacitor with automatic recharging, which provides the necessary electrical current pulse up to 500 A at a voltage of 12 V to actuate the blade. The sensors system of the striker position is installed on the striker guide and is a system of slit type fast-acting photo-light emitting diode (LED) optical sensors.

Special ridges on the striker block the light beam, ensure positioning of the striker relative to the sample. The system assumes armed state when striker tip initially impacts the surface of the specimen. After the striker bounces 0.1 mm from the specimen surface, an electric impulse is transmitted to the electromagnet, which activates the cut-off blocking system.

The system is connected to the network and its state is monitored by the indicators. The position of the cut-off blade relative to the striker is rechecked after the sample is placed on the working table. The position is corrected by adjusting nuts located in the lower part of the guides if necessary. The impactor position sensor operation is checked immediately before the experiment by placing a 0.1 mm thick gauge between the impactor and the test object. Control photo-LED of the sensor must lit up following the placed gauge detection.

The dent depth is denoted by d and refers to the residual depth of the defect formed by the impactor after impact. The dent depth can be defined as the maximum distance in the direction perpendicular to the specimen surface from the lowest point of the dent to the plane of the impacted surface. Dent depth measurement within 15 minutes after the tests, as well as 7 days after the moment of testing, was carried out on a special clamming device, which consists of a rigid supported base, identical to the upper support bed of the unit with a similar cut-out. This support fixture is characterised by a simpler and quicker anchorage of the specimen after it has been impacted (Fig. 2.14). The depth of indentation on the surface of the specimens is measured with a dial indicator type gauge after impact.

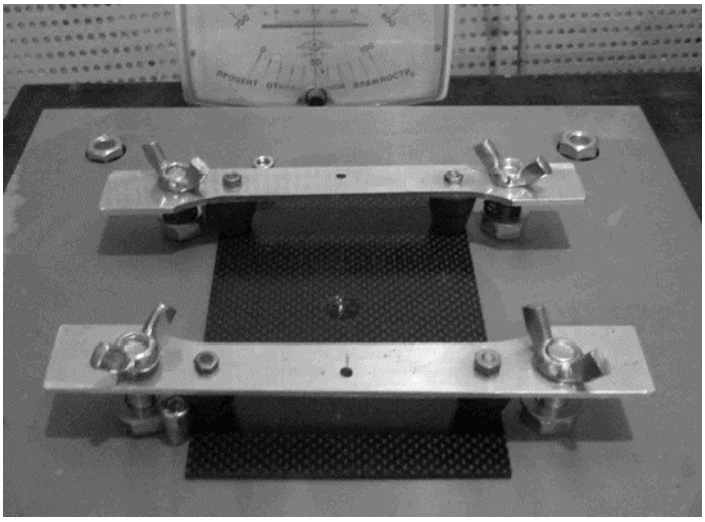

Fig. 2.14. Support Fixture.

2.4. Means of measurement data collection

The test implementation required the use of accurate measuring instruments and special measuring systems including measuring devices. The accurate measurement of linear geometric dimensions of samples (length and width), as well as other dimensions and distances up to 150 mm was done using a 31C628 TOREX calliper with a measurement error ±0.02 mm (<100 mm) and ±0.03 mm (>100 mm). Thicknesses in the specified locations was measured using a MK-25 No.9412 micrometre (Fig. 2.15).

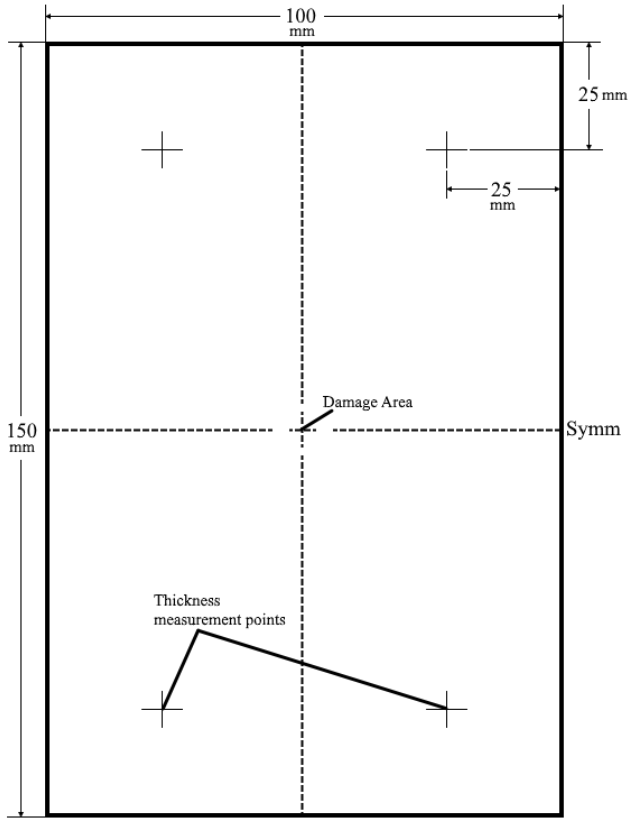

Fig. 2.15. Dimensions and measurement points of CFRP plate.

All measuring instruments used were certified for compliance of measured values with reference values with a given accuracy class and had valid certification. To properly measure the thickness a special conductor was attached to one end piece (Fig. 2.16). The specimen was inserted into this conductor and the thickness of the specimen was measured at the thickness measurement points.

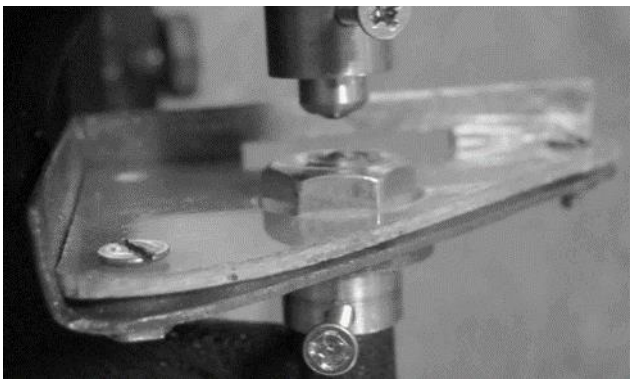

Fig. 2.16. Clammed micrometre conductor.

According to the standard, the pressing force of the gauge head should be at least 120 kg, therefore, in order to ensure the specified pressing force of each head in each measuring instrument, preliminary tests were carried out. The size of the pressure heads together with rubber tips amounted to 26.4±0.2 mm. The reduction in size for the different heads amounted to values in the range of 23.3÷23.6 mm after pressing the head with a pressure screw against the carbon fibre plate under which the dynamometer was located.

The measuring system for determining the drop height of the striker included a calliper, gauge (Fig. 2.17a) and a spacer (Fig. 2.17b).

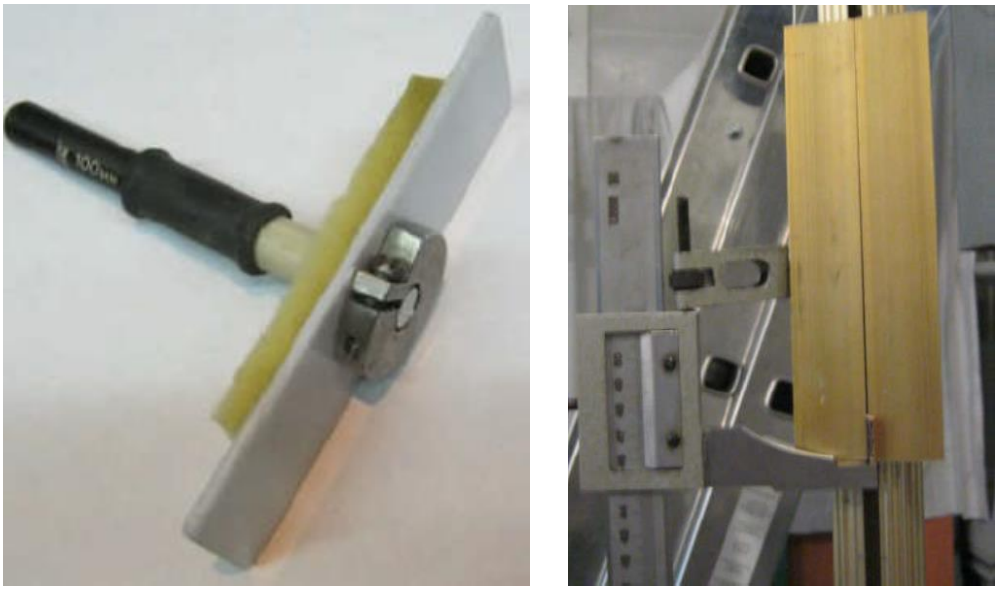

(a) (b)

Fig. 2.17. Gauge (a) and spacer (b).

The 180 mm long spacer is a T-shaped profile consisting of 2 identical angles, allows to fix drop height H by wedging in the vertical tube slot at a certain height set by means of a calliper. If the height of the drop is greater than 800 mm, which exceeds the total range of the calliper, gauge and spacer (100 + 520 + 180) mm, the digital calliper 31C628 TOREX was used in addition.

Measurement of the depth of the indentation on the surface of the samples after the impact was carried out by a special measuring device - depth gauge. Which has the form of a funnel with an outer diameter of 65 mm and the width of the supporting ring edging 2 mm. Before the measurements, the indicator was fixed with the help of a screw in such a way

that the indicator reached the maximum value of 2 mm. On the polished surface, a level was set on the indicator using a special adjustment screw, which corresponded to zero indentation of the sample surface. After applying this measuring device to the dent, the position with the maximum value was found.

The exact mass of the falling weight in this research was determined with the help of MIRTA scales (Fig. 2.18). As a result of measurements the mass of the impactor with shank was determined to be 2.248 kg, which was used in further studies to determine the load drop height. This impactor mass is near the limit of the standard recommended mass range of 2±0.25 kg.

Fig. 2.18. Scales.

The testing of the specimens must be performed under a standard laboratory atmosphere (23±3 °C and 50±0% relative humidity).

The temperature in the testing area and relative humidity were measured using a combined device barothermohygrometer BM-2.

The samples must also be kept under these conditions for at least 40 hours before testing. In order to ensure the specified test conditions, a special computerised climate control chamber was developed, which consists of two units, namely a thermal stabilisation unit and a special computerised control system unit (Fig. 2.19).

Fig. 2.19. Climate control chamber.

A 25 W regulated electric heater with was used as a heating element in the climate control chamber. Air circulation in the chamber was provided by a fan. Temperature regulation was provided by switching the heating element on and off by means of a computerised control system unit with a semiconductor temperature sensor. Temperature control and switching on of the heating element is indicated on a digital LED indicator. The control buttons on the digital indicator set the minimum temperature at which the heating element is switched on and hysteresis - temperature increase to the minimum temperature at which the system switches off the heater, then the system switches to fully automatic operation mode.

Repeated control of temperature in the climate control chamber and on the surface of samples, carried out with the help of infrared thermometer, showed the temperature variation inside the climate control chamber 22,4 - 24,1 °C shown in Fig. 2.20.

Fig. 2.20. Temperature control using infrared thermometer.

Conclusion to the Part 2

The selection of impact-resistant materials for this study was based on the manufacturer's declaration of their resistance to impact. An FE model impact simulation was performed to compare with experimental results. The FE model created in Abaqus software using explicit-dynamic finite element solver. Mechanical material that were taken into account are listed in the table 2.1 in chapter 2.1. To obtain experimental data, the drop tower provided by NAU Department of Mechanics laboratory was utilized. The testing installation features: automatic blocking system, trigger lock and special clamming device, making it optimal for preforming experimental studies. The dimensional parameters were measured manually with certified measuring tools to ensure minimal error.

PART 3. EXPERIMENT RESULTS AND DISCUSSION

This part mainly focuses on experimental and simulation results, arising discrepancies and restrictions as well as post impact residual strength investigation.

The drop test execution included the following stages. Firstly, the research methodology was developed, then, the drop tower was prepared, the metrological certification of equipment and instruments was carried out to conduct experimental studies on the damage caused by the impact of falling weight and confirm the results obtained. Experimental results were then compared to simulation data.

The damaged specimens had been used for post impact compression tests to determine their residual strength. During loading, the dependence of the applied force on the stroke of the piston rod of the testing machine was recorded. All studies were carried out on specimens provided by Antonov Enterprise.

3.1. Testing procedure

For mechanical impact experimental study, a systematic procedure was employed. Initially, specimens underwent a climate 40 hours control procedure, conducted in laboratory atmosphere conditions (23±3 °C and 50±10% relative humidity). This pre-testing climate control involved placing specimens, housed in a specialized conductor, within a heat stabilization chamber. Subsequently, the thickness of each specimen was meticulously measured at four corner points, positioned 25 mm away from both sides of the specimen, using a micrometre equipped with a special conductor. The average of these measurements was calculated and considered as the specimen thickness - t. The impact energy was then determined using the equation 2.1:

$$E = C_E t \text{ [J]}, \tag{2.1}$$

where: E - potential energy of the striker before impact, C_E - is the specified ratio of impact energy to specimen thickness 6.7 [J/mm], t - nominal thickness of the specimen [mm].

Striker drop height H was determined using this equation:

$$H = E/m_d g \text{ [m]}, \tag{2.2}$$

where m_d - mass of the impactor [kg], g - free fall acceleration 9.81 [m/s^2].

Initially, the specimen was positioned on the upper support of the rigid base support and precisely aligned over the rectangular cutout, using three rubbered clamps. The striker position was aligned with the centre of the CM coupon, secured at drop height H by the trigger lock.

Subsequently, the blocking system was engaged. The striker was dropped onto the specimen by activating the mechanical trigger lever. The absence of a repeated impact was monitored and the specimen was carefully extracted without touching the backside.

Visual assessment of damage was recorded, detailing the type and maximum dent diameter on the front D_f and back side D_b of the specimens. Following this, the specimen had been fixed in place for dent depth measurement d_0, conducted within 15 minutes after the test, using a dial-type measuring device.

Additional measurements included the depth of the dent d_7 seven days after the initial impact and calculating the degree of damage relaxation within seven days η using the specified equation 2.3:

$$\eta = \frac{d_0 - d_7}{d_0} 100\%, \quad (2.3)$$

where d_0 - dent depth determined within 15 minutes after the test, d_7 – dent depth 7 days later.

The measurement results were then recorded and compiled.

3.2. Comparative analysis of experimental and simulation results

The results presented in table 3.1 exhibit a significant discrepancy between dent depths of simulated impact and real experiment. Meanwhile, simulated impact deformation pattern based on Antonov and Hexcel material catalogue mechanical properties data regularly match, although in some cases (1.1, 5.1) Hexply based models appear to be more tough.

Table 3.1

Experimental Results

									Dent depth			Maximum dent size		Simulation	
#	Material	l, mm	w, mm	tav, mm	Ce E1, J/mm	E=E1*t, J	H=E/mg, mm	V, m/s	d_0, mm	d_7, mm	η, %	D_f, mm	D_b, mm	d_{FE}, mm	d_h, mm
1.1	913/35%/UD132/HTS-12K	100	150	2.16	4.47	9.335	423.5	2.8818	0.10	0.09	14.8	5.75	37.9	0.341	0.140
1.2	913/35%/UD132/HTS-12K	100	150	2.19	6.7	14.67	665.6	3.6127	0.945	0.90	4.44	12.90	103.5	0.413	0.412
1.3	913/35%/UD132/HTS-12K	100	150	2.18	6.7	14.64	664.1	3.6090	0.91	0.80	11.2	12	94.8	0.413	0.412
2.1	913/46%/G18NT	100	150	2.98	6.7	19.98	906.4	4.2161	3.09	2.28	26.2	16.3	44.4	0.473	0.473
2.2	913/46%/G18NT	100	150	3.06	6.7	20.52	930.8	4.2727	2.84	2.48	12.7	16	46.4	0.478	0.478
3.1	M21/40%/268T2/AS4C-6K	100	150	2.60	6.7	17.47	792.5	3.9424	0.79	0.612	22.6	12.8	31.4	0.446	0.445
3.2	M21/40%/268T2/AS4C-6K	100	150	2.57	6.7	17.25	782.6	3.9175	0.95	0.84	10.8	11.3	36.1	0.444	0.443
4.1	M21/34%/UD194/IMA-12K	100	150	3.04	6.7	20.37	923.9	4.2570	0.21	0.132	35.9	33	42	0.478	0.478
5.1	M21/34%/UD268/AS7-12K	100	150	2.12	6.7	14.20	644.3	3.5543	0.72	0.62	14.2	10.3	77.8	0.482	0.407
5.2	M21/34%/UD268/AS7-12K	100	150	2.14	6.7	14.39	652.7	3.5780	0.61	0.54	12.0	9.86	72.8	0.411	0.409

Prominently, the dent dept measured 15 minutes after impact and simulation results are illustrated below (Fig. 3.1, Fig 3.2).

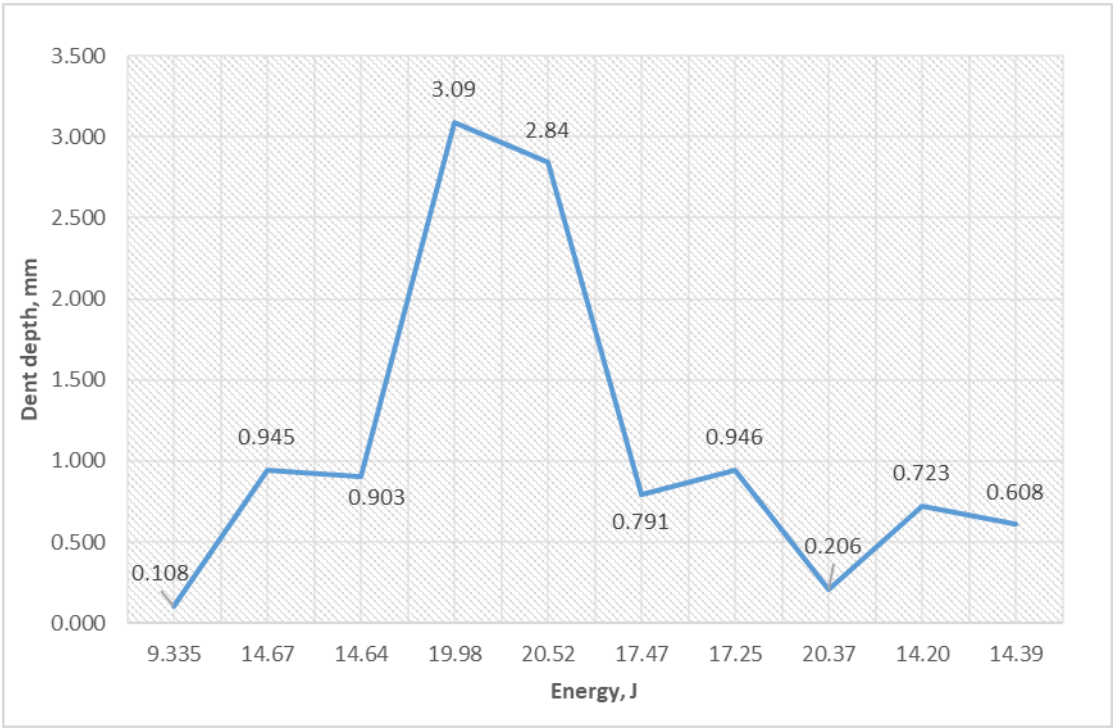

Fig. 3.1. Experimental dent depth

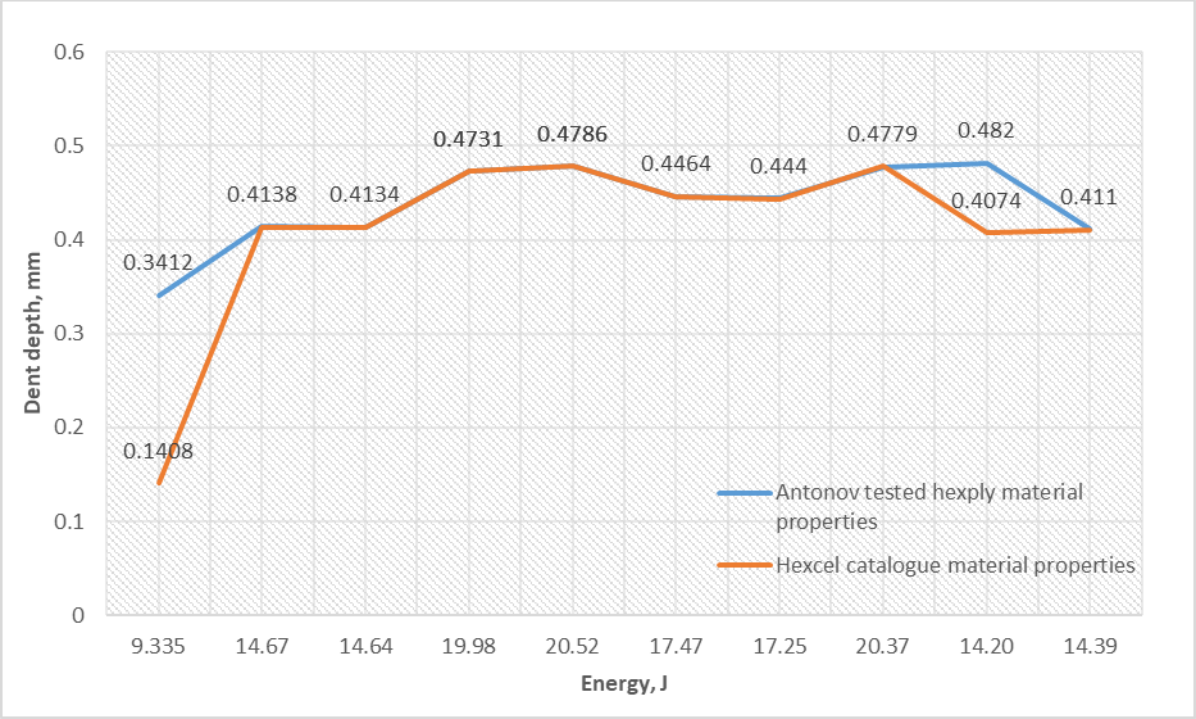

Fig. 3.2. Simulated dent depth.

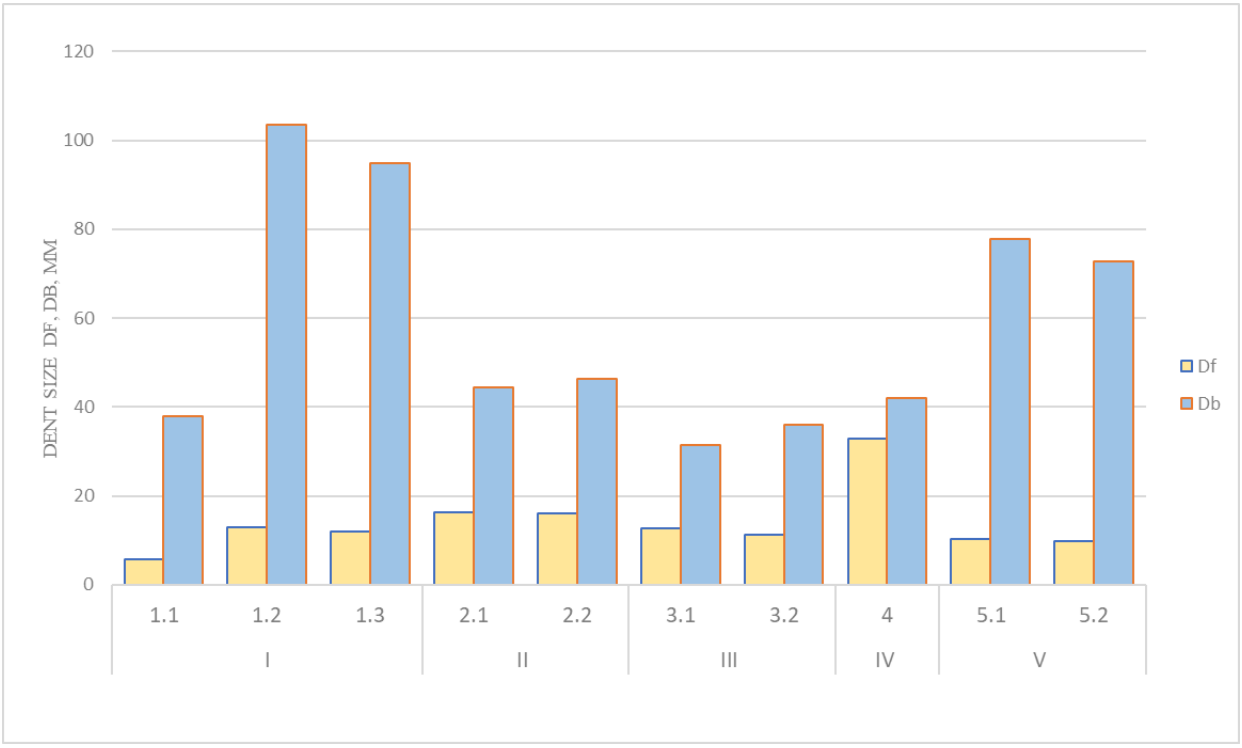

Fig. 3.3. Histograms of dent diameters of front side D_f and the back side D_b.

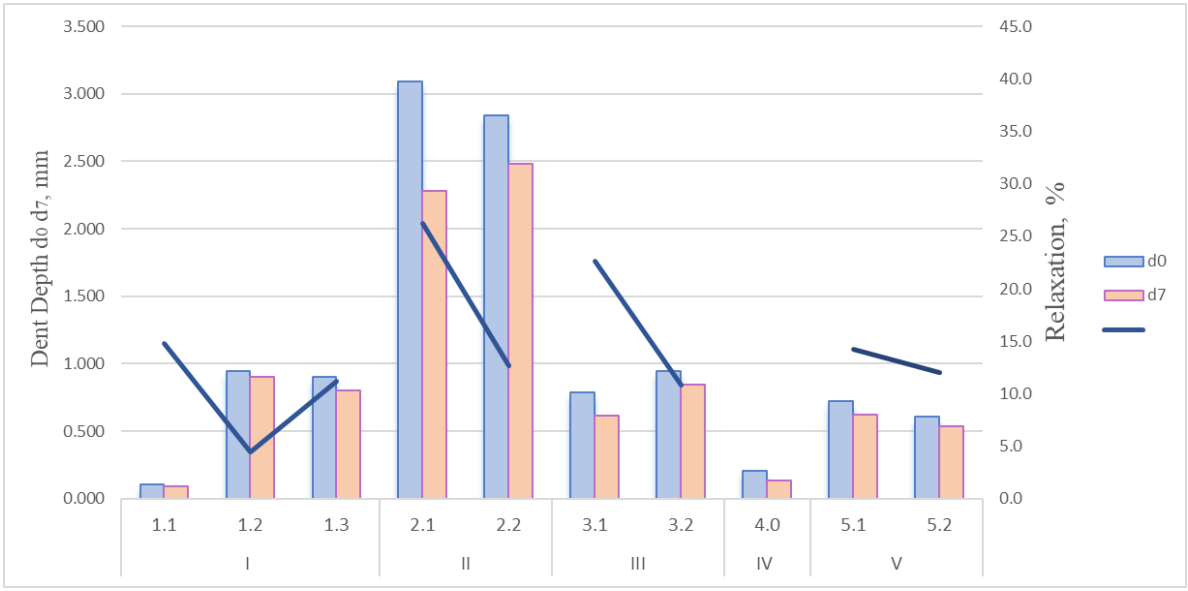

Fig. 3.4. Histograms of dent depth measurements immediately after impact d_0 and 7 days post d_7 with damage relaxation curves.

In a directly related study, samples of carbon fibre reinforced plastics based on M21 epoxy resin and two different filler structures (bidirectional fabric and unidirectional carbon tape) were also subjected to low-velocity impact testing. Damage parameters and relaxation were investigated. The research results were presented in the form of similar histograms of dent depths and damage diameters from both sides of the samples [26].

Interestingly the FE model internal stresses appear to somewhat resemble the post impact dent severity. Fig 3.3 includes (from left to right): principal stresses of FE model based on Antonov provided material properties and Hexcel catalogue as well as images of front and back side of impacted specimens.

1.1

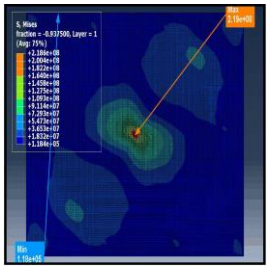
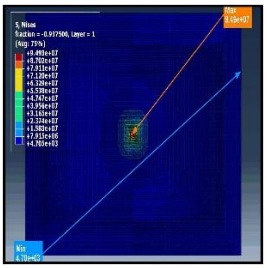
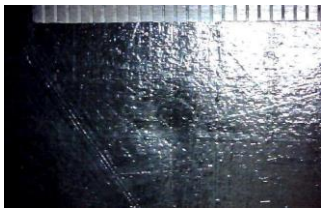


1.2

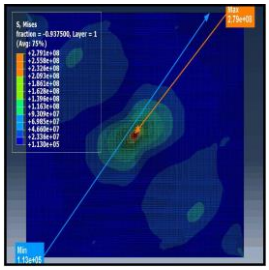
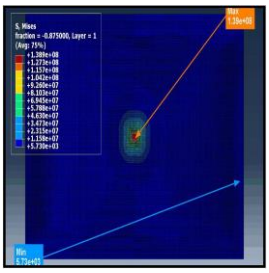
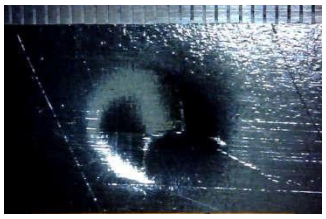


1.3

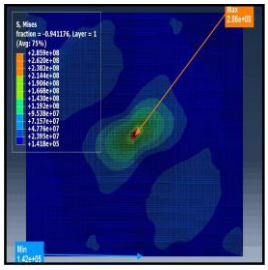
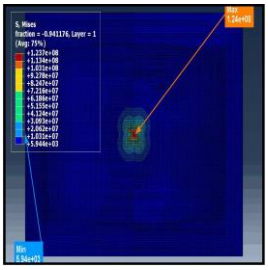
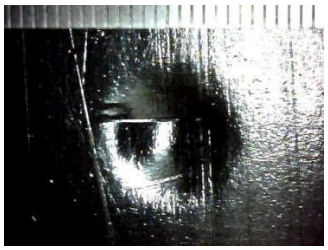


2.1

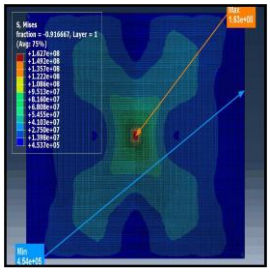
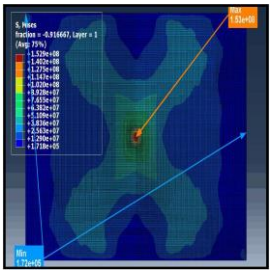
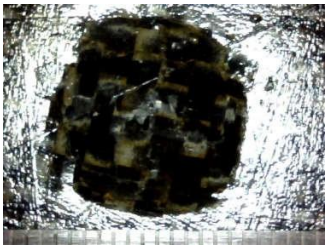
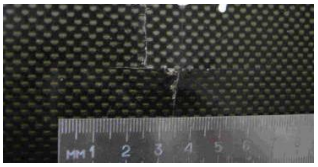

2.2

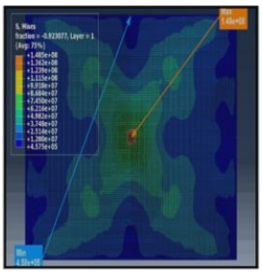
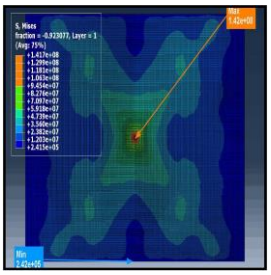
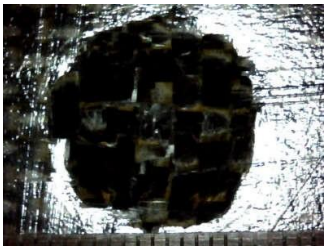
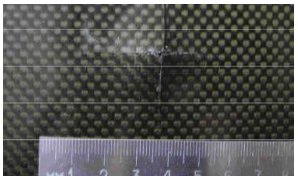

3.1

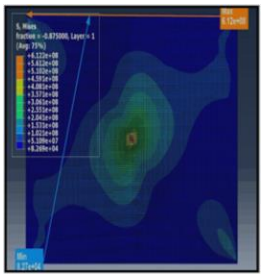
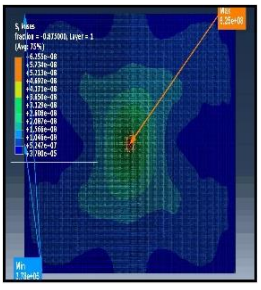
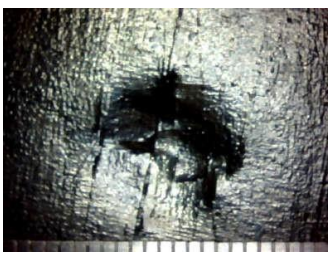


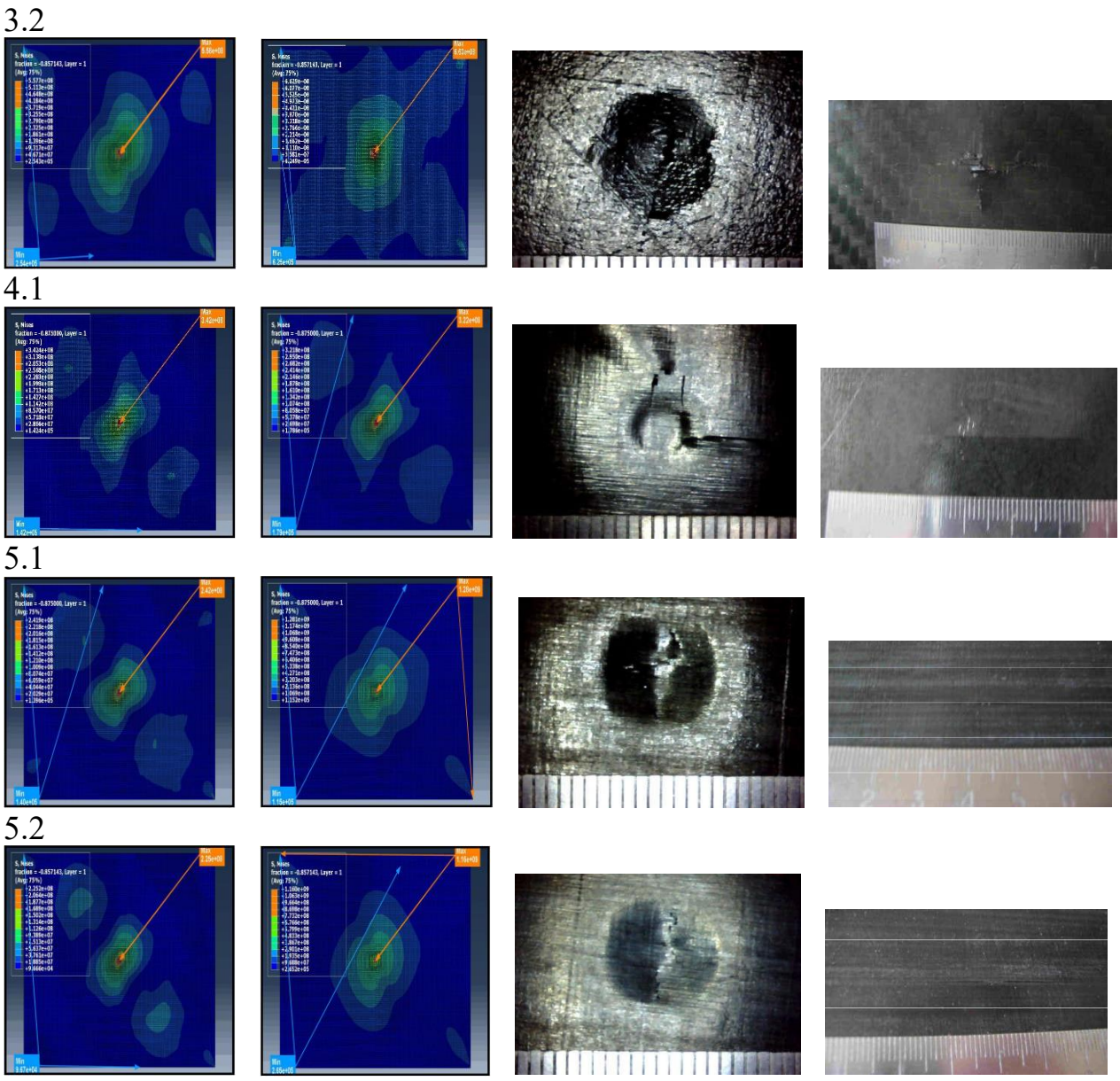

Fig. 3.5. Simulation principal stress and experimental indentation.

Displacement values are included in Appendix.

As a result of testing the produced damage could not be classified as BVID (table 3.2), i.e. one that is not detectable by external visual inspection by an operator with 100% natural or optically corrected visual acuity from a distance of 0.7 m under directional or under illumination of the specimen. Therefore, all of the following specimens were tested at a typical impact energy of 6.7 J/mm. Classification of visible surface damage:

I – indentations;
II – crack/chip;
III – crack/delamination combinations;
VI – dent/crack/delamination combinations.

Table 3.2

Damage Classification Of Tested CFRP

#	1.1	1.2	1.3	2.1	2.2	3.1	3.2	4.1	5.1	5.2
Damage Type	I	IV	IV	IV	IV	IV	IV	IV	IV	IV

The following limitations and inaccuracies were identified in the modelling process playing into divergence of data. The amplitude or the energy change rate was not recorded during the experiment so was ultimately unavailable. The falling velocity therefore impact energy was simulated as a constant output. The drop tower and rubbered clamps properties were not included, instead set as a clammed boundary condition. Several Hexcel catalogue material properties were missing and replaced with Antonov data to make the simulation possible, therefore tainting the credibility of the results. The time frame of impact was restricted by the calculation limit. And finally, the striker did not perform a bounce releasing tension. Further assessment reveals that the dent depth and dimensions are dependant on material relaxation while tested specimens were subjected to rest time, the simulation was performed instantly and recorded and the highest possible deformation values.

Experimental drop test analysis conducted by Tita, de Carvalho and Vandepitte (2008) verified by ultrasonic C-scan employed a finite element model and UMAT subroutine implemented into software ABAQUS to simulate the failure mechanisms of the composite laminate. The contact time depends on the impact energy level; so, the contact time was longer for specimens impacted by impact energy of 2.36 J than by impact energy of 5.91 J. Thus, for high contact time, the mechanical behaviour of the specimen tended to be quasi-static. However, the specimens impacted by 2.36 J had only absorbed 1.2 J of energy, converting 50% of the impact energy to elastic vibrations. Thus, the specimens impacted by 2.36 J have shown less failure mechanisms [27].

Related study has shown the increase in the diameter of the impactor led to an in-plane damage decrease along with the predicted through-thickness gradual decrease. This is reasonable since the equivalent impact energy is applied and a lower impactor diameter leads to more localized damage [28].

3.3. Assessing post-impact effects on compressive strength and mechanical properties degradation in carbon fibre reinforced plastics

The failure modes demonstrated by carbon-fibre reinforced composite laminates can be generally divided into two categories: interlaminar failure, characterized by delamination, and intralaminar failure, which includes matrix cracks and fibre pull-out/breakage. Impact damage has the potential to affect various aspects of laminates, including buckling, compressive strength, tensile strength, and fatigue life. The most substantial reductions typically occur in compressive properties, studies on tensile strength after impact have been constrained, as the effect is less significant compared to compression.

While the impact location seems to have a relatively minor impact on damage width as long as it is far from a boundary, damage widths increase for impacts near a boundary due to reduced flexibility, leading to less elastic energy absorption [22].

The failure modes presented by carbon-fibre reinforced composite laminates may be broadly classified into two categories: interlaminar (delamination) and intralaminar (matrix cracks and fibre pull-out/breakage) failure. It is readily observed that the higher the initial impact damage, the greater the stiffness and compressive strength reduction [29].

Compression after impact entails a complex interplay between compressive failure, and local and global buckling. The compressive failure strain is markedly influenced by impact location, damage geometry, boundary conditions, and the extent of fibre fracture.

The results of impact tests revealed that natural or hybrid composites exhibited greater absorption of impact energy compared to glass/epoxy composites, primarily attributed to extensive impact damages. Conversely, natural fibre composites displayed the lowest compression during CAI tests. The conclusion drawn was that natural fibre or hybrid composites demonstrate higher specific compressive strength values when compared to glass/epoxy composites. The alteration of stacking sequences had a significant impact on post-impact performance. Incorporating natural fibres in the exterior led to a reduction in glass fibre breakages, resulting in notably higher residual compressive strength values, particularly at higher impact energies [30, 31]. Meanwhile, in another study the woven laminate exhibited the highest compression strength across all impact energies, attributed to its reinforcement architecture controlling damage spread. In contrast, quasi-isotropic

laminates demonstrated superior damage tolerance, with the smallest normalized strength reduction at all tested impact energies, possibly due to protective surface plies safeguarding the load-bearing 0° plies against impact damage unlike cross-ply laminates where 90° plies provided least stiffness [32]. An equation for estimating the residual strength after impact by measuring the size of the permanent impression that remains on the surface of composite materials after impact is proposed in this study [33].

The optimization of Carbon Fibre Reinforced Polymer (CFRP) materials for enhanced performance under impact loading and subsequent compression tests has become a focal point in ensuring the structural integrity and longevity of CFRP aerospace parts. Material selection, fibre architecture design, and the incorporation of interlaminar toughening mechanisms as well as strategies such as employing hybrid composites, surface protection methodologies, matrix modifications or nano particle injection, [34] advanced manufacturing techniques, and post-cure processing are explored to enhance the overall damage tolerance of CFRP. Furthermore, structural design optimization and the utilization of continuous monitoring systems contribute to a comprehensive framework aimed at mitigating the effects of impact events and improving the resilience of CFRP structures in the face of CAI testing.

Conclusion to the Part 3

Based on testing data: carbon fibre reinforced plastic based on bidirectional carbon fabric, when subjected to an impact with the same energy of 6.7 J per 1 mm thickness, exhibits an average 10% reduction of dent depth (d_0) compared to carbon fibre reinforced plastic based on unidirectional carbon tape. On the back side, the dent diameter (D_b) for both types of carbon fibre reinforced plastics is significantly larger compared to the diameter D_f on the front side. Specifically, for carbon fibre reinforced plastic based on bidirectional fabric, the difference is 2.8 times, while for carbon fibre reinforced plastic based on unidirectional tape, the difference is more than 5 times. The dent diameter on the back side (D_b) for carbon fibre reinforced plastic based on bidirectional fabric on average is 1.8 times less than that of carbon fibre reinforced plastic based on unidirectional tape. The reduction in dent depth (d_0) over a weekly period, also known as relaxation, for carbon fibre reinforced

plastic based on bidirectional fabric averages 18.1%, whereas, for carbon fibre reinforced plastic based on unidirectional tape, it is 15.4%, approximately 1.2 times smaller.

The discrepancy in experimental results and simulations arises from the limitations of the model: constant amplitude, missing rubbered clamps properties, missing material properties, time frame calculation limit restriction, no bounce back.

PART 4. LABOR PROTECTION

4.1. Introductory definitions

1. A health hazard is a factor which under certain conditions leads to illness and lowers performance efficiency of an employee.

2. A safety hazard is a factor, the impact of which, under certain conditions, leads to injury or other sudden health deterioration of an employee.

Fillers and polymer binders used in the production of PCM are usually classified as hazardous, flammable and explosive substances. Therefore, it is necessary to carefully follow all special safety, labour protection and fire prevention instructions while handling PCM.

The rules apply to the following technological processes:

- resin formulation;
- material cutting;
- manufacturing or preparation of prepregs or fabric resin impregnation;
- manual hand layup of prepregs, automated fibre placement or manual fibre layup;
- moulding (vacuum bag curing, resin transfer or infusion moulding, in and/or out of autoclave curing);
- machining;
- testing;
- quality control.

All of the above must be carried out in specially designated or separated areas at the workshop or a laboratory [35].

The feature common to all composite processes is combining resin, a curing agent, some type of reinforcing fibre, and in some cases a solvent. Typically, heat and pressure are used to shape and cure the mixture into a finished part. Solvents may serve three purposes:

- as part of the resin mixture;
- as part of the process;
- as a cleaning agent for removing residue from the process equipment. [36]

4.2. Dangerous byproducts of composite material moulding

The resin biners used in composite manufacture have high molecular weights with low vapor pressures, therefore they possess decreased volatility as stated in OTM. Epoxy resin system components have very low vapor pressures and they are not present as a volatilized airborne hazard. Nevertheless, the dangers of CM manufacture components are presented in table 4 [36].

Table 4

Health Hazards Of CM Components

Composite component	Organ system target (possible target)	Known (possible) health effect
Resins		
Epoxy resins	Skin, lungs, eyes	Contact and allergic dermatitis, conjunctivitis
Polyurethane resins	Lungs, skin, eyes	Respiratory sensitization, contact dermatitis, conjunctivitis
Phenol formaldehyde	Skin, lungs, eyes	As above (potential carcinogen)
Bismaleimides		
Polyamides		
Reinforcing materials		
Aramid fibres	Skin (lungs)	Skin and respiratory irritation, contact dermatitis (chronic interstitial lung disease)
Carbon/graphite fibres		
Glass fibres (continuous filament)		
Hardeners and curing agents		
Diaminodiphenylsulfone	-	No known effects with workplace exposure
Methylenedianiline	Liver, skin	Hepatotoxicity, suspect human carcinogen
Other aromatic amines		
Meta-phenylenediamine	Liver, skin (kidney, bladder)	Hepatitis, contact dermatitis (kidney and bladder cancer)
Aliphatic andcyclo-aliphatic amines	Eyes, skin	Severe irritation, contact dermatitis
Polyaminoamide		Irritation (sensitization)
Anhydride	Eyes, lungs, skin	Severe eye and skin irritation, respiratory sensitization, contact dermatitis

Machining or finishing of coupons or working parts are required in many PMC involved processes: manufacture or experimentation. Typical finishing methods involve grinding, drilling, sanding or manual touch-up work. All equipment in use must be in full serviceability and its condition constantly monitored by the by the technical management. It is necessary to ensure that the workpieces are securely fastened, which largely depends

on the condition of the axis centres and centre holes of the machining tool [37].

The most common byproduct of any touch up work is highly volatile dust containing traces of fibres. Although, some particles are considered respirable, the most likely effect of long term exposure to carbon black is chronic lung disease [38]. Studies of some graphite-epoxy finishing operations found respirable fractions ranging from 25% to 100%.

Investigation of the ability of carbon nanoparticles to affect the integrity of the blood-brain barrier as well as exhibit chemical effects within the brain have shown that nanoparticles can overcome this physical and electrostatic barrier to the brain. In addition, high concentrations of anionic nanoparticles and cationic nano particles are capable of disrupting the integrity of the blood-brain barrier [39]. Therefore a proper ventilation and exhaust system must be installed throughout the facility.

4.3. Personal means of protection and work ethic

Workplace personal protective equipment (PPE) must be chosen specifically and be appropriate for the component in use. Typical PPE involves double layered nitrile-fabric gloves, protective suit (non woven fabric, dust and water resistant materials), and eye protection (glasses with side shields, goggles, face shields).

Generally, the resins are of a larger molecular size and so are less likely to permeate protective materials than the curing agents and solvents. The aromatic amine curing agents are particularly difficult to protect against, according to OTM.

Respiratory protection is as strongly enforced in many advanced or automated composites manufacture processes, due to the low vapor pressure of the materials involved. However, respiratory protection is necessary at sites with improper ventilation (increased airborne solvent levels, dust levels), inadequate climate control, limited workspace which leads to several processes transpiring concurrently involving exposed hand work and resin missing (machining).

Due to constant exposure to toxic materials workplace controls are essential to ensure safe and reliable and continuous operation of any production, testing or experimental facility. The various types of workplace controls found in the advanced composite workplace are engineering controls and work practice involving the appropriate layout and

workshop supervision mainly by isolating storage, controls.

Engineering controls involve separating process areas, segregating enclosures, installing local exhaust ventilation and fire suppression systems. Most dangerous byproduct of resin or fibre combustion is toxic smoke [40].

Binder components: assorted resins and curing agents must be kept in a designated controlled and ventilated area under certain temperature to maintain initial properties. Personal equipment and instruments must be stored separately to minimize cross-exposure. Finishing tools, machines, testing systems any other electrical equipment must undergo frequent maintenance and hold valid certification. Production processes should transpire in logical succession, independently with minimum risk of sabotaging one, another approximate example (no definitive production technology): material quality control must be done before preparation and cutting, cutting section must not directly neighbour the layup bench, curing process and machining of products must be performed in different sections, post curing and/or machining sample testing must be conducted in a non-contaminated designated area.

The main focus of work practice controls is human centred, established to enforce a certain work ethic. Fundamental and easily implemented work practices used to minimize exposures to harmful materials used in composite production are frequent briefings about personal safety as well as good employee training and education, adherence to procedure manuals for production, process and control equipment, proper use, maintenance, and cleaning of personal protective equipment, personal hygiene program and spending time outdoors [41], periodic inspections and maintenance of production, process and control equipment, adequate supervision.

Production areas exceeding 500 m^2 are classified as explosion-hazardous and are required to be equipped with automated fire suppression systems. Areas under 500 m^2 must feature a fire alarm system integrated with primary firefighting equipment. The workshop must include specific fire protection provisions, such as panels equipped with necessary firefighting equipment and the placement of two fire extinguishers per 600 m^2 of facility space. Moreover, equipment for prepreg production (impregnation machines) should be equipped with a fire suppression system responsive to critical temperature elevations within

drying chambers [42].

The formulation of the Occupational Safety Instruction adheres to the "Regulations on the Development of Occupational Safety Instructions," as endorsed by the State Labor Inspectorate of Ukraine through Order No. 9 dated January 29, 1998. Its primary objective is to ensure secure working conditions during the fabrication of components from composite materials.

Key general safety requirements for working with CM include the following:

- admission of individuals aged 18 and above and only after prior medical assessment, occupational safety orientation, familiarization with the technological instructions, and past certification (retraining occurs no less than quarterly);
- provision of specialized attire, footwear, and personal protective equipment for personnel involved in composite material work;
- equipping production premises with interchangeable inlet-exhaust ventilation systems, providing workbenches with local exhaust systems;
- proper storage of adhesives, solvents, and binders in hermetically sealed, coloured metal containers, adhering to conditional markings and quantities within daily limits;
- mandatory wet cleaning within production premises twice per working shift;
- prohibition of welding operations and open flame use within premises dedicated to composite material part fabrication;
- adherence to labour protection requirements specified in regulatory enactments governing machinery, mechanisms, equipment, and other production facilities, with mandatory use of personal protective equipment. Compliance with labor protection requisites outlined in the collective agreement and internal work schedule of the enterprise is obligatory (Article 18 of the Law of Ukraine "On Labor Protection") [43].

4.4. Laboratory setting precautions

The previously listed workplace controls apply in experimental composite material coupon level testing laboratories or sites. That being said, any person that working in a

laboratory must receive specific training from their department and/or supervisor. [44]. Typical laboratories contain sections designated for explicitly testing the samples and result processing areas. The first section is made up of various universal or tensile, peeling, shear, flexural, compression, impact, fatigue testing machines and their corresponding processing units. Result processing area includes a sitting workspace and a personal computer to generate reports.

Individuals engaged in testing procedures are required to wear appropriate protective equipment, adhere to the guidelines outlined in machine manuals. Face protection such as safety glasses or face shields, to guard against potential splinters or debris accumulating from the destruction of materials. Lab coats and gloves serve as an additional layer of defence from any potential harm or contaminants preventing direct contact with exposed materials. Apart from a ventilation system, used to maintain a clean and safe laboratory environment, the testing site must be supplied with fire suppression means in the form of foam (flammable liquids, combustible materials), carbon dioxide (electrical equipment, flammable liquids) and dry powder (electrical equipment, flammable gasses, metals, liquids) extinguishers [45]. Much like the laboratory where impact testing of samples has been performed.

Conclusion to the Part 4

Pre-emptive awareness of the dangers of components used in production or testing of CM parts is indispensable in ensuring a secure and productive working environment. From the initial handling of raw materials to the intricate processes of production and subsequent testing, the use of personal protective equipment and workplace controls is essential. However many developing CM production sites or fully fledged facilities may neglect or simply not follow the regulations due to financial instability or ignorance. Thus the responsibility of one’s well-being can rest directly on the employee, even if they are ill-equipped or the workplace does not facilitate engineering workplace controls adequately. Awareness of the hazards and harmfulness of materials among staff and management plays a crucial role in conducting successful tests and quality production.

PART 5. ENVIRONMENTAL PROTECTION

This part critically assesses the environmental impact of integration of composite materials in the aviation industry. The lightweight and high-strength attributes of composites have redefined aircraft design, promising fuel efficiency gains, however the ecological consequences are yet to be fully assessed. The composite industry is dedicated to creating resolutions that not only enhance the quality of life and comfort for individuals, but also mitigate the socio-environmental effects of composite goods. Such a goal mandates an approach that considers the entire lifecycle of the composite product, from its inception in manufacturing to its ultimate disposal. Products that are both environmentally-friendly and valuable to consumers will continue to be in demand.

5.1. Environmental impact of composite materials

Compared to conventional materials, composites exhibit a diminished environmental impact due to utilization of low-emission manufacturing methods. Composite materials are also a more sustainable option because their production takes less energy. Composite materials are safe and environmentally friendly because they don’t contain any harmful elements and don’t discharge dangerous chemicals into the atmosphere [46]. Although, mass production facilities often employ in-autoclave curing process and generate waste due to scrapped parts.

Despite the operational advantages of these materials, the CM parts in the aircraft structure also have disadvantages. Technological differences in composites and metals in the context of airline incidents and used aircraft construction materials, heat performance in aircraft fire during an aircraft incident is an important issue. Fires involving composite materials can release toxic fumes and microparticles into the air, causing health risks. On the basis of the flammability tests, it was found that carbon-fiberglass hybrid composite with a foam core, was least favourable for both flammability and fume release. Making it evident that the extraordinary events and incidents of CM aircraft have a negative impact not only on the air, but significantly damage the environment at the place of the event [47].

The disposal and recycling of composite parts pose considerable challenges within

the broader context of sustainable materials management. The inherent difficulty arises from the irreversible curing process during composite manufacturing, rendering the fibres immovably integrated into the matrix. Consequently, the reclamation of individual fibres becomes a formidable task, hindering effective recycling efforts. Furthermore, the non-biodegradable nature of composite materials exacerbates environmental concerns, particularly when these components are destined for landfills. The disposal of cured composite parts in landfills not only contributes to the accumulation of non-recyclable waste but also raises ecological apprehensions due to their extended persistence and potential leaching of harmful substances.

The laboratory testing of composite structures within the aviation industry necessitates a discerning examination of its environmental implications. While the immediate impact is less pronounced than in the operational phase, considerations include the responsible utilization of materials throughout testing processes. The generation and disposal of composite specimens, including unused or discarded materials, the use of chemicals and coatings in testing procedure, the powering of testing equipment contributes to the laboratory's overall carbon footprint.

5.2. Recycling and disposal of composites

Composite recycling efforts in the past mainly concerned grinding, shearing, chipping, or flaking the composite into suitable size to be used as filler material in new moulded composite parts. However, composite aircraft parts usually contain valuable carbon fibre and resins, and in order to efficiently extract and recycle these components, other recycling processes must be used [48].

Recent years have seen improvements made in composites recycling. There are now more options for the disposal and recycling of composite materials including mechanical, thermal, fluidized, pyrolysis and chemical recycling.

The process of mechanical recycling entails cutting the composite material into smaller pieces and powdering it, the powder can then be used a filler. In thermal recycling, the composite material is heated to a high temperature, the resin is broken down, and the reinforcing fibres are recovered and may be used again. Chemical recycling includes

disassembling the composite material's resin component into its individual chemicals, resins can then be reused [49]. Pyrolysis is a thermal depolymerisation at high temperatures in the absence of oxygen, allowing for the recovery fibres. It can be used for the treatment of polymers and polymer matrix composites Fluidized-bed recycling process developed at the University of Nottingham is used to combust the resin matrix as energy and to recover the glass or carbon fibres. [50] In total three composites recycling technologies cover 75% of the total research activity: pyrolysis (31%) and solvolysis (22%) and mechanical grinding (18%). These three technologies dominate the picture of recycling, however in many instances combining mechanical grinding with another technology took place according to [51].

The recycled fiberglass fibres been effective in reducing shrinkage in concrete thereby increasing its durability and as a filler in resin or civil engineering structures.

Recycled carbon fibres are used in bulk moulding compounds for smaller, non load-bearing components, as a sheet-moulding compound and as recycled materials in load-bearing shell structures. It can be found in phone cases, laptop shells and even water bottle cages for bicycles [52].

The unique characteristics and significant potential of sub- and supercritical fluids can enhance various chemical processes involving diverse materials. The adoption of these fluids holds promise for replacing environmentally harmful solvents, particularly prevalent organic solvents, within industrial applications. Carbon fibre recycling has been a notable application of various sub- and supercritical fluids, including water, methanol, ethanol, propanol, and acetone. Consequently, high-pressure technologies employing sub- and supercritical fluids present opportunities to produce novel products with specific properties or design environmentally friendly and sustainable processes.

Efficient and rapid resin degradation has been reported using sub- and supercritical fluids due to their enhanced properties, including a liquid-like high mass transport coefficient, pressure-dependent solvent power, and gas-like low viscosity and high diffusivity. The density of sub- or supercritical fluids can be easily manipulated by slight variations in pressure and temperature. While viscosity is relatively low, it may increase with temperature, and surface tension is essentially non-existent. The high diffusivity

induces intriguing transport phenomena in condensed phases. Recent applications of sub- and supercritical fluids in technological realms have focused on developing green processes, categorizing them as green reaction media due to their cost-effectiveness, ready availability, and low potential toxicity. Moreover, these fluids can be recycled through distillation and are capable of dissolving numerous organic and inorganic compounds.

In addition to dissolving organic materials, sub- and supercritical fluids can permeate porous solids, which remain relatively benign under atmospheric conditions. These fluids prove to be excellent reaction media for the depolymerization or decomposition of polymers, exhibiting fast and selective reactions. Composite materials, such as carbon fibre-reinforced composites, can undergo decomposition into smaller molecular components and fibre materials. Although the use of catalysts is not imperative, their inclusion significantly enhances the decomposition reaction [53].

At the same time, thermosets unlike thermoplastics cannot be reprocessed due to the formation of permanent cross links during curing; therefore, the waste ends up in landfills. Landfills use up vast amounts of land and contribute to the greenhouse effect by emitting landfill gas which contains carbon dioxide, methane, volatile organic compounds, hazardous air pollutants and odorous compounds that can adversely affect environment. Gases that are associated with landfills have been linked to cancer and respiratory diseases. [50]. Simultaneously, incineration disposal of any carbon fibre containing product is not recommended due to possible oxidation of carbon fibres leading to the creation of small-diameter fibres which could also be carcinogenic. Additionally, the presence of carbon fibres in the airstream can result in shorting within electric flue gas filters in incinerators. Consequently, if recycling proves unfeasible for waste carbon fibre composite materials, the preferred alternative is landfill disposal. Therefore if waste carbon fibre composite material cannot be recycled it is recommended to send to landfill [54].

Conclusion to the Part 5

The recyclability of composite materials is influenced by factors such as the type of resin, the reinforcing material, and the manufacturing process. Choosing an appropriate recycling technique depends on the specific type of composite material in question.

Thermoset polymer resins, commonly contain volatile organic compounds and are non-biodegradable often end on landfill escalating the problem further. CM samples used for mechanical testing are usually thermosets which makes disposal challenging as the fibres cannot be retrieved. The best recycling solution for destroyed samples would be mechanical grinding and subsequent use of residue powder in adjacent production facility.

GENERAL CONCLUSION

In this work, CFRP samples made from unidirectional and fabric Hexcel prepregs were subjected to low-velocity impact testing, and impact damage simulation based on experimental and catalogue material properties. The experimental results were processed and the depth and diameter of dent damage on both sides of the specimen were determined. Additionally, for the first time, the material relaxation over a weekly period of the dented specimens was assessed.

Carbon fibre reinforced plastic specimens based on bidirectional fabric prepreg showed a 10% reduction in dent depth (d_0) compared to unidirectional carbon tape samples, both impacted with an energy of 6.7 J per 1 mm thickness. On the back side, dent diameter (D_b) for bidirectional fabric CFRP was 1.8 times smaller on average than that of unidirectional tape CFRP samples. The dent diameter D difference between the front (D_f) and back sides (D_b) for bidirectional fabric CFRP was 2.8 times, and for unidirectional tape CFRP, it exceeded 5 times. Over a week, the relaxation in dent depth (d_0) was 18.1% for bidirectional fabric CFRP and 15.4% for unidirectional tape CFRP, approximately 1.2 times smaller.

An extensive impact simulation has been performed using Abaqus/Explicit software. However, the FE simulation model does not sufficiently reflect the development of residual stresses in the material, due to processing reaching a calculation limit within the given time frame and no bounce back. Despite these drawbacks, the study allowed for the assessment of CFRP properties and revealed that materials based on bidirectional fibre exhibit better resistance to impact damage and a higher degree of relaxation.

The subsequent studies of post-impact relaxation are necessary as damages caused by it are challenging to detect, especially Barely Visible Impact Damage (BVID). However, the front may side may show a dent these damages are more pronounced on the back side, leading to a reduction in the compressive strength of the composite material due to delamination and fibre bond breakage.

REFERENCES

1. ASTM 7136/D7136M, Standard test method for measuring the damage resistance of a fiber-reinforced polymer matrix composite to a drop-weight impact event – 2012, p4.

2. Israr H. A., & Hongkarnjanakul N., Rivallant S., Bouvet C. Post-Impact Investigation of CFRP Laminated Plate. // Jurnal Teknologi. – №71. – 2014.

3. Safri S.N.A., Sultan M.T.H., Yidris N., and Mustapha F. Low Velocity and High Velocity Impact Test on Composite Materials – A review // The International Journal Of Engineering And Science (IJES). – №3(9). – 2014. – p. 50-60.

4. Mathivanan R., Jerald, J. Experimental investigation of low-velocity impact characteristics of woven glass fiber epoxy matrix composite laminates of EP3 grade // Materials & Design. – №31. – 2010. – p. 4553-4560.

5. Ghasemnejad H., Soroush V.R., Mason P.J., Weager B. To improve impact damage response of single and multi-delaminated FRP composites using natural Flax yarn // Materials and Design. – №.36. – 2012. – p. 865-873.

6. Pernas-Sanchez J., Pedroche D.A., Varas D., Lopez-Puente J., Zaera R. Numerical modeling of ice behavior under high velocity impacts // International Journal of Solids and Structures. – №49. – 2012. – p. 1919–1927.

7. Lessard L., Hosseinzadeh R., Shokrich M. Damage behavior of fibre reinforced composite plates subjected to drop weight impacts // Composite Science and Technology. – № 66. – 2006. – p. 61-68.

8. Cantwell, W.J. and Morton, J. The impact resistance of composite materials - a review // Composites – № 22(5). – 1991. – p.347-362.

9. Eltaher M.A., Basha M., Wagih A., Melaibari A., Lubineau G. On the impact damage resistance and tolerance improvement of hybrid CFRP/Kevlar sandwich composites // Microporous and Mesoporous Materials. – №333(3). – 2022.

10. Wu H.-Y.T., Springer G.S. Measurements of matrix cracking and delamination caused by impact on composite plates // Journal of Composite Materials. – №22. – 1988. – p.518-532.

11. Doxsee L.E., Rubbrecht P., Li L., Verpoest I., Scholle M. Delamination growth

in composite plates subjected to transverse loads // Journal of Composite Materials. – №27(8). – 1993. – p.764-781.

12. Budhoo Y., Liaw B., Delale F., Iyer R., Raju B. Temperature effect on drop-weight impact of hybrid woven composites // ASME-IMECE Conference. – Vancouver, British Columbia, Canada, November 12-18, 2010.

13. Richardson M.O.W., Wisheart M.J. Review of low-velocity impact properties of composite materials. Institute of Polymer Technology and Materials Engineering, Loughborough University of Technology, Loughborough, Leicestershire LEll 3TU, UK (Received 28 October 1994; revised 19 April 1996), p6.

14. Wang B., Zhong S., Lee T., Fancey K., Mi J. Non-destructive testing and evaluation of composite materials/structures: A state-of-the-art review. // Advances in Mechanical Engineering – №12. – 2020.

15. Panettieri E., Fanteria D., Montemurro M., Froustey C. Low-velocity impact tests on carbon/epoxy composite laminates: A benchmark study // Composites Part B: Engineering. – №107. – 2016 – p. 9-21.

16. Bogenfeld R., Gorsky C. An experimental study of the cyclic compression after impact behavior of CFRP composites // Journal of Composites Science. – №5. – 2021.

17. Destic F., Bouvet C. Impact damages detection on composite materials by THz imaging //Case Studies in Nondestructive Testing and Evaluation. – №6, – 2016. – p.53–62.

18. Francis D. Non-Destructive Evaluation (NDE) of Polymer Matrix Composites. A volume in Woodhead Publishing Series in Composites Science and Engineering. – Elsevier. 2013. – 692 p.

19. Strag M., Swiderski W. Non-destructive inspection of military-designated composite materials with the use of terahertz imaging // Composite Structures. – №306. – 2023.

20. Strag M., Swiderski W. Defect detection in aramid fiber-reinforced composites via terahertz radiation // Journal of Nondestructive Evaluation. – №42. – 2023.

21. Paipetis A., Katerelos, D. Post-Impact-Fatigue behaviour of composite laminates: Current and novel technologies for enhanced damage tolerance // Composite Laminates: Properties, Performance and Applications. – 2010. – p. 1-82.

22. Olsson R. Strength of composite laminates after impact: background and recommendations // Swerea. – 2011. – p. 1-17.

23. [Electronic resource] HexPLy M21 Global Data Sheet – Access Mode: https://hexcel.com/user_area/content_media/raw/HexPly_M21_global_DataSheet.pdf.

24. [Electronic resource] HexPLy M21 Global Data Sheet – Access Mode: https://hexcel.com/user_area/content_media/raw/HexPly_M21_global_DataSheet.pdf.

25. Ali A., Sanuddin A., Yee H.B., Afshar R. Simulation of an impact test for PC-PET plastic // Recent Trends in Fracture Mechanics. – 2012. – p.127-139.

26. Шевченко О.А., Рогожина Н.О. Параметри та релаксація пошкоджень від низькошвидкісного удару вуглепластиків з різними структурами наповнювача // Матеріали XVI міжнародної науково-технічної конференції «АВІА-2023». – Київ: НАУ, 18-20.04.2023. – С. 1.70-1.74.

27. Tita V., de Carvalho J., Vandepitte D. Failure analysis of low-velocity impact on thin composite laminates: Experimental and numerical approaches // Composite Structures. – №83. –2008. – p. 413–428.

28. Yang B., Chen Y., Lee J., Fu K., Li Y. In-plane compression response of woven CFRP composite after low-velocity impact: Modelling and experiment // Thin-Walled Structures. – №158. – 2021.

29. Liu H., Falzon B. G., Tan W. Predicting the Compression-After-Impact (CAI) strength of damage tolerant hybrid unidirectional/woven carbon-fibre reinforced composite laminates // Composites Part A: Applied Science and Manufacturing. – №105. – 2018. – p. 189-202.

30. Selver E., Dalfi H., Yousaf Z. Investigation of the impact and post-impact behaviour of glass and glass/natural fibre hybrid composites made with various stacking sequences: Experimental and theoretical analysis // Journal of Industrial Textiles. – №51. – 2020.

31. Im K.H., Sim J.K., Yang I.Y. Impact damages and residual bending strength of CFRP composite laminates subjected to impact loading // KSME Journal. – №10. – 1996. – p. 423–434.

32. Sanchez-Saez S., Barbero E., Zaera R., Navarro C. Compression after impact of

thin composite laminates // Composite Science and Technology. – №65(13). – 2005. – p. 1911-1919.

33. Koo J-M., Choi J-H., Seok C-S. Prediction of residual strength of CFRP after impact // Composites Part B: Engineering. – №54. – 2013. –p.28-33.

34. Saghafi H., Fotouhi M., Minak G. Improvement of the impact properties of composite 2 laminates by means of nano-modification of the matrix-A review // Applied Sciences. – № 8. – 2018.

35. Колінченко Д. О. Дослідження впливу співвідношення компонентів на властивості полімерної матриці. Магістерська дипломна робота. Національний університет «Запорізька політехніка». 2020.

36. Polymer Matrix Materials: Advanced Composites. OSHA Technical Manual (OTM). – Section III: Chapter 1. Access mode: https://www.osha.gov/otm/section-3-health-hazards/chapter-1 (last access 17.11.2023). – Title from the screen.

37. Геворкян Е. С., Тимофеєва Л. А., Нерубацький В. П. та ін. Інтегровані технології обробки матеріалів : підручник. – Харків: УкрДУЗТ, 2016. – 238 с.

38. Carbon Black. Wisconsin Department of Health Services. Access mode: https://www.dhs.wisconsin.gov/chemical/carblack.htm#:~:text=The%20most%20likely%20effect%20of,lodge%20deep%20in%20their%20lungs (last access 17.11.2023).

39. Oberdorster G., Maynard A., Donaldson K., Castranova V., Fitzpatrick J., Ausman K., Carter J., Karn B., Kreyling W., Lai D., Olin S., Monteiro-Riviere N., Warheit D., Yang H.. Principles for Characterising the Potential Human Health Effects from Exposure to Nanomaterials: Elements of a Screening Strategy // Particle and fibre toxicology. – №2(8). – 2005.

40. Mouritz A. P., Gibson A. G. Health Hazards of Composites in Fire. In: Fire Properties of Polymer Composite Materials. – Dordrecht.: Springer. Solid Mechanics and Its Applications. – №143. 2006. – 401 p.

41. Barclay R., Webber S., Ripat J., Grant T., Jones C. A., Lix L. M., Mayo N., van Ineveld C., Salbach N. M. Safety and feasibility of an interactive workshop and facilitated outdoor walking group compared to a workshop alone in increasing outdoor walking activity among older adults: a pilot randomized controlled trial // Pilot and Feasibility Studies. –

№4(179). – 2018.

42. Савченко І. М. Підвищення технологічних властивостей природних композиційних матеріалів. Магістерська дипломна робота. Національний університет «Запорізька політехніка». 2020.

43. Крюковська О. А., Литвинова Є. Е. Заходи безпеки у виробництві композиційних матеріалів на основі епоксидних та фенолформальдегідних смол // Енергетика: економіка, технології, екологія. № 3. – 2019. – С. 104-109. – Режим доступу: http://nbuv.gov.ua/UJRN/eete_2019_3_14.

44. Alaimo P., Langenhan J., Tanner M., Ferrenberg S. Safety Teams: An Approach To Engage Students in Laboratory Safety // Journal of Chemical Education. – №87. – 2010.

45. Ziegler-Rodriguez K, Margallo M, Aldaco R, et al (2020). Types of fire extinguisher. Surrey Fire & Safety Ltd. Access mode: https://surreyfire.co.uk/types-of-fire-extinguisher/ (last access 17.11.2023).

46. Environmental Benefits of Composite Materials. Composites Fiberglass International. – May 24, 2023. Access mode: https://cfint.com.au/environmental-benefits-of-composite-materials/#:~:text=Compared%20to%20conventional%20materials%2C%20composite,energy%20and%20emits%20fewer%20emissions (last access 17.11.2023). – Title from the screen.

47. Vajdova I., Jencova E., Szabo S. Jr., Melnikova L., Galanda J., Dobrowolska M., Ploch J. Environmental Impact of Burning Composite Materials Used in Aircraft Construction on the Air // International Journal of Environmental Research and Public Health. – №16(20). – 2019.

48. Composite Recycling and Disposal An Environmental R&D Issue. Boeing Environmental Technologies. – Volume 8, Number 4, November 2003. Access mode: https://www.boeingsuppliers.com/environmental/TechNotes/TechNotes2003-11.pdf (last access 17.11.2023). – Title from the screen.

49. Recycling and Disposal of Composite Materials. Composites Fiberglass International. – Feb 2, 2023. Access mode: https://cfint.com.au/recycling-and-disposal-of-composite-materials/ (last access 17.11.2023). – Title from the screen.

50. Vijay N., Rajkumara V., Bhattacharjee P. Assessment of Composite Waste Disposal in Aerospace Industries // Procedia Environmental Sciences. – №35. – 2016. – p. 563-570.

51. Rybicka J., Tiwari A., Leeke G. Technology readiness level assessment of composites recycling technologies // Journal of Cleaner Production. – №112(1). – 2016.

52. Johnson, Todd. Recycling Composite Materials. Thought Co. – Aug. 05, 2018. – Access mode: https://www.thoughtco.com/recycling-composite-materials-820337 (last access 17.11.2023). – Title from the screen.

53. Borjan D., Knez Z., Knez M. Recycling of Carbon Fiber-Reinforced Composites-Difficulties and Future Perspectives // Materials. – №14(15). – 2021.

54. What Can I Do With My Waste? Composites UK, Trade Association. Access mode: https://compositesuk.co.uk/industry-support/environmental/what-can-i-do-with-my-waste/ (last access 17.11.2023). – Title from the screen.

APPENDIX

Deformation along Z axis

Antonov Tested | Hexcel Catalogue

1.1

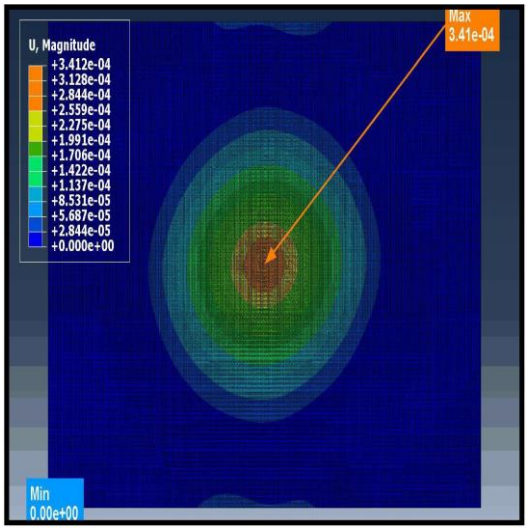

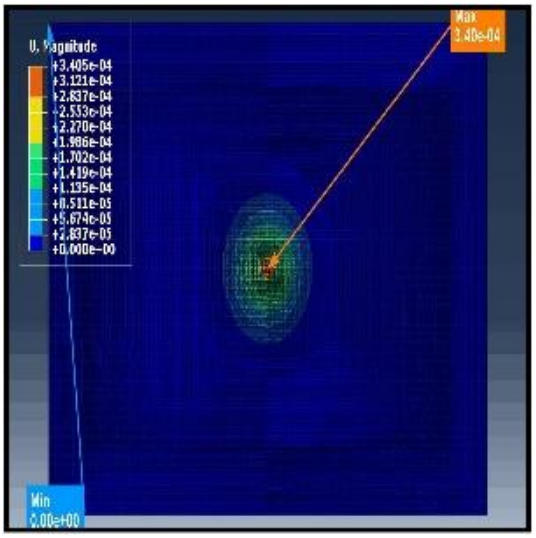

1.2

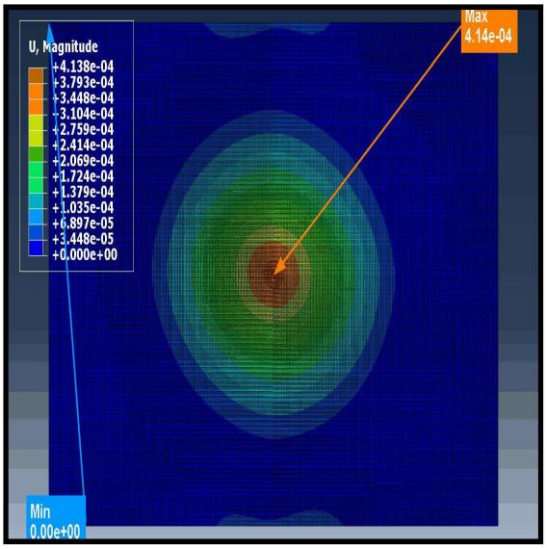

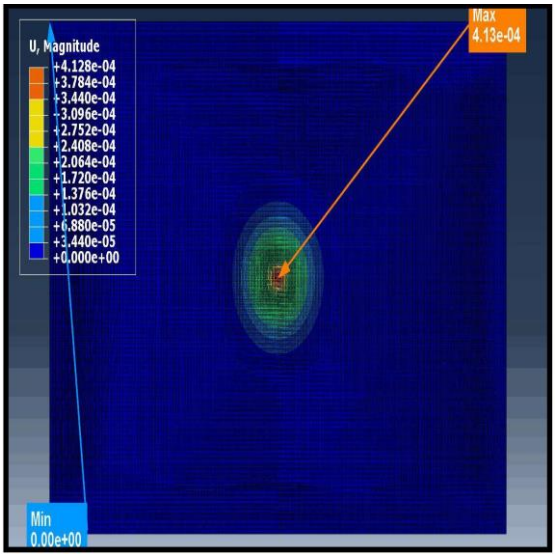

	Antonov Tested	Hexcel Catalogue
1.3	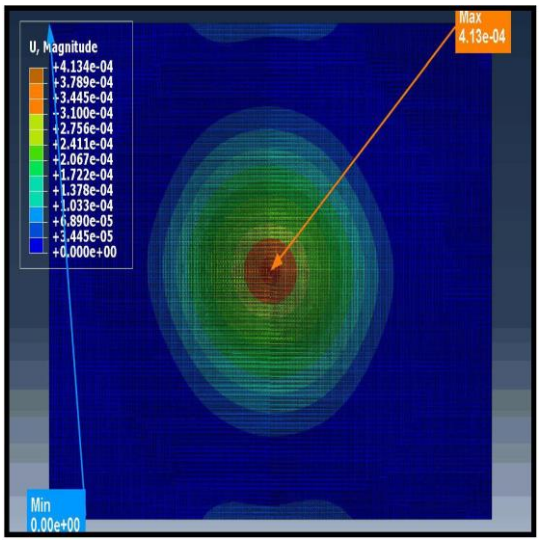	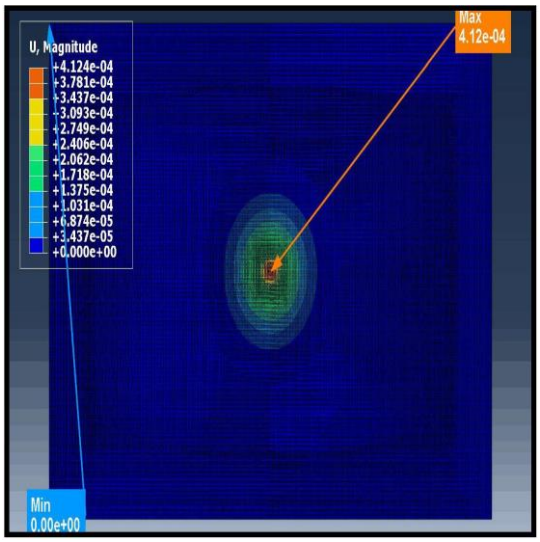
2.1	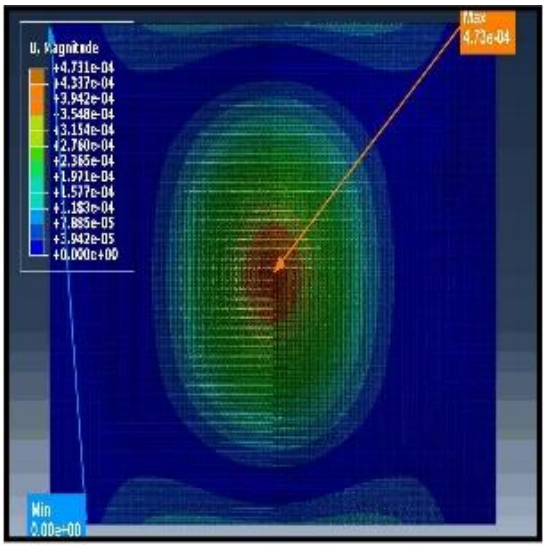	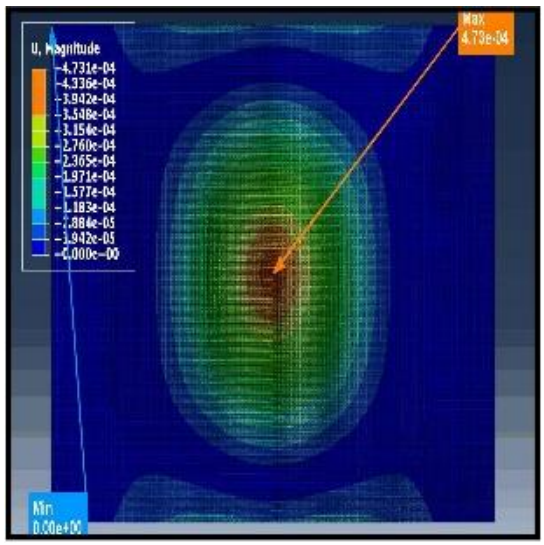
2.2	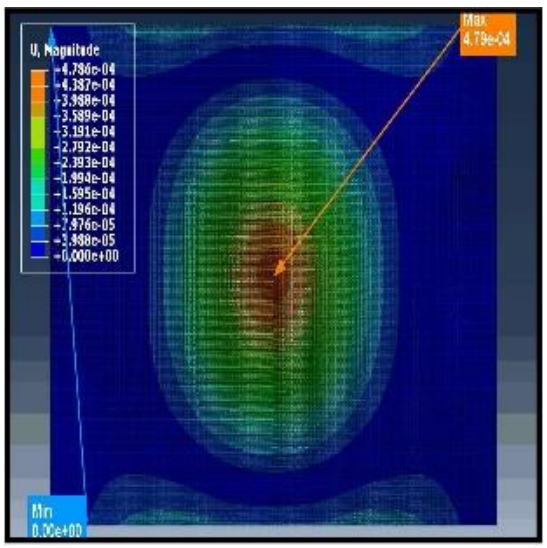	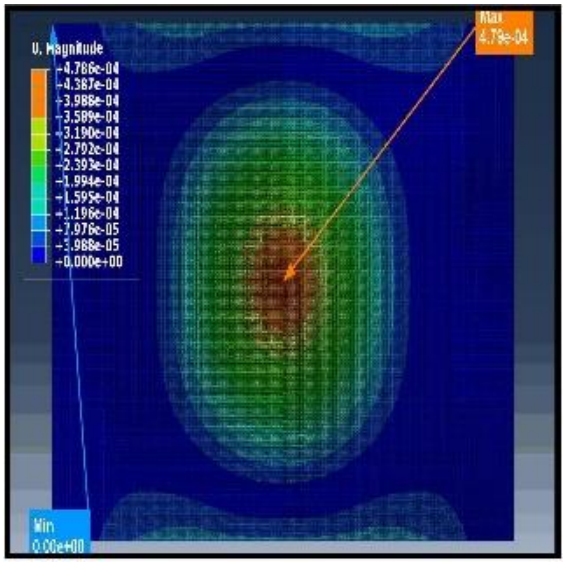

	Antonov Tested	Hexcel Catalogue
3.1	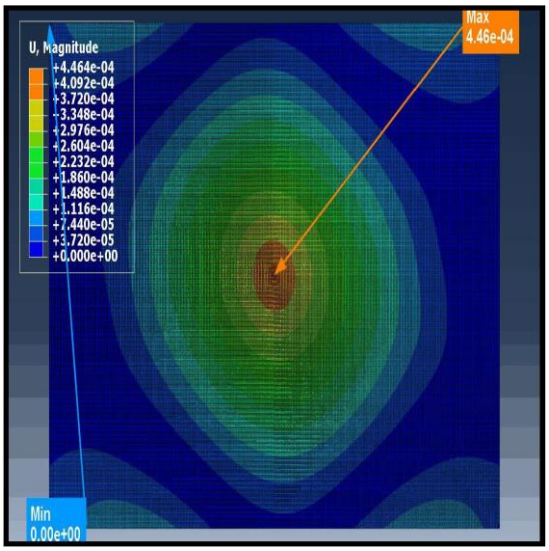	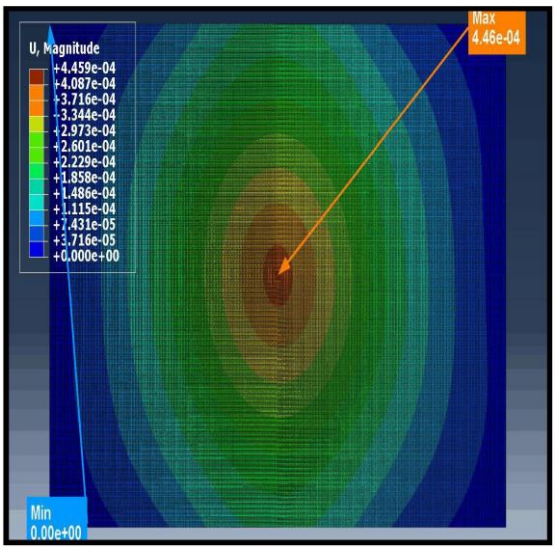
3.2	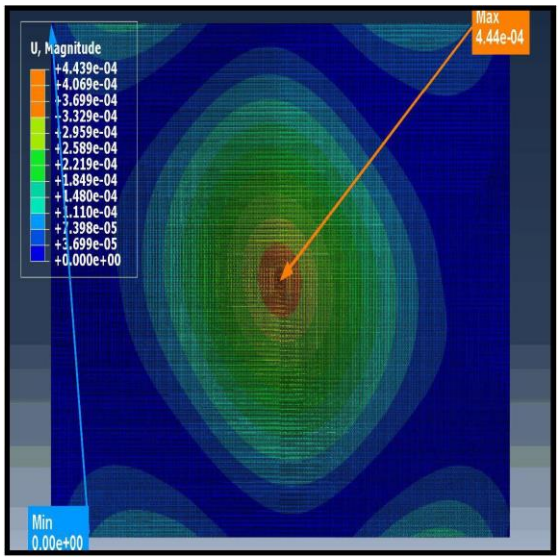	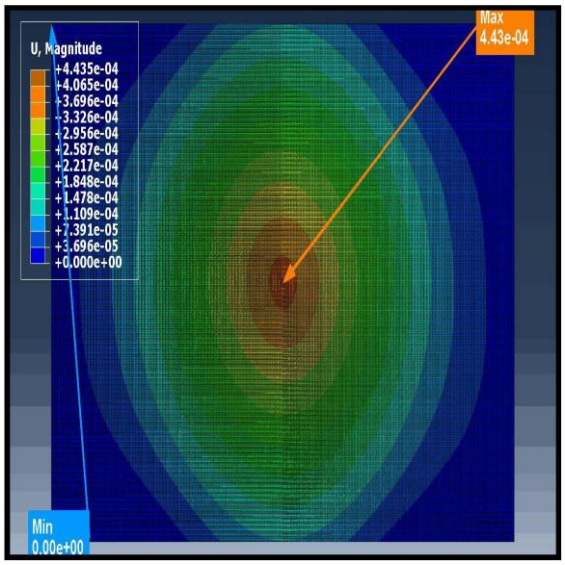

	Antonov Tested	Hexcel Catalogue
4.1	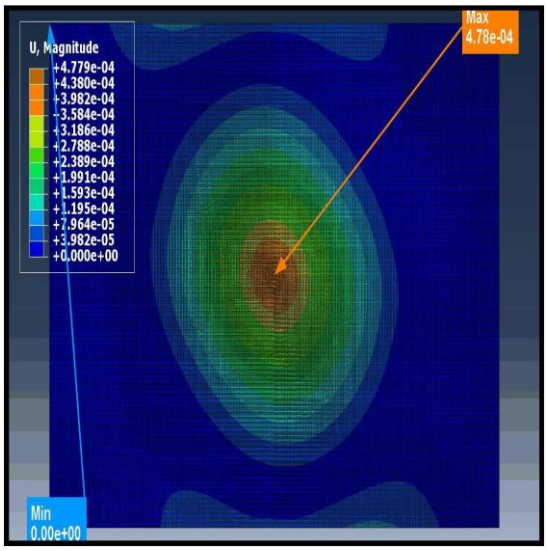	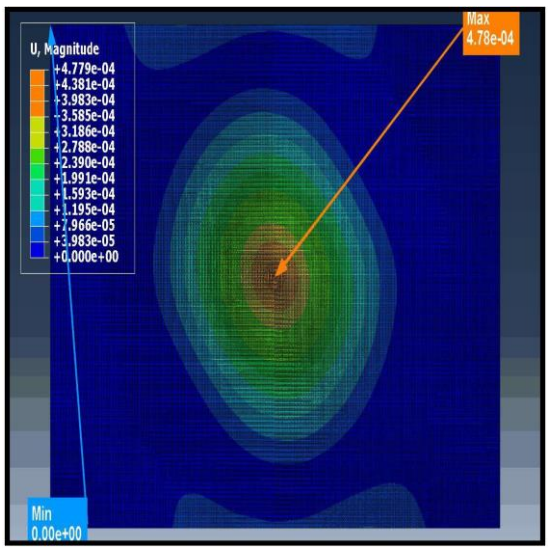
5.1	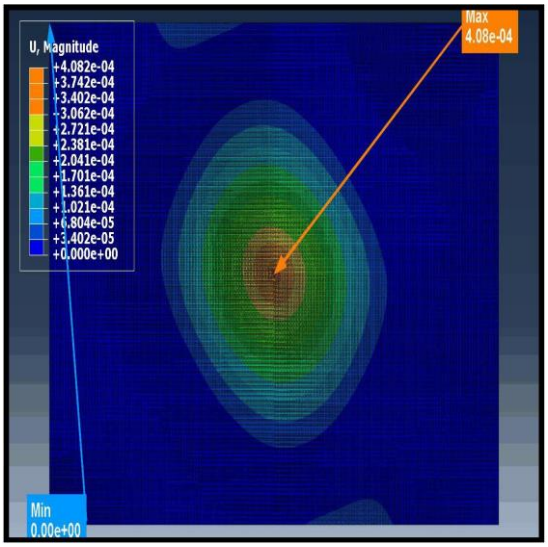	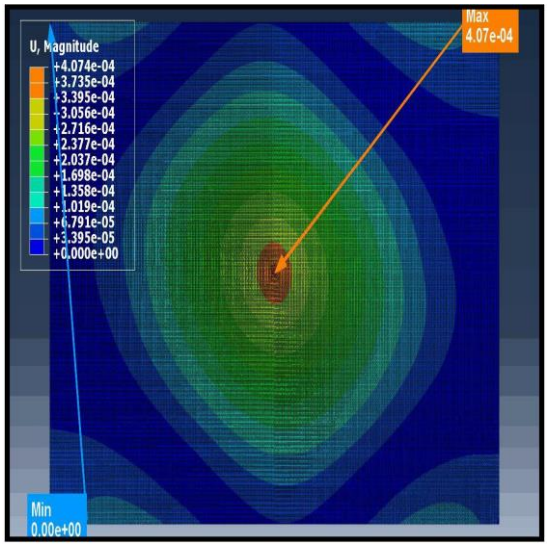
5.2